E- 5592

N 70 23430

NASA TECHNICAL MEMORANDUM

NASA TM X-52769

NASA TM X-52769

PRELIMINARY PERFORMANCE OF A BRAYTON-CYCLE-POWER-SYSTEM GAS LOOP OPERATING WITH KRYPTON OVER A TURBINE INLET TEMPERATURE RANGE OF 1200° F TO 1600° F

by Alfred S. Valerino, Robert P. Macosko,
Armen S. Asadoruian, Thomas P. Hecker
and Roman Kruchowy
Lewis Research Center
Cleveland, Ohio
March 1970

This information is being published in preliminary form in order to expedite its early release.

PRELIMINARY PERFORMANCE OF A BRAYTON-CYCLE-POWER-SYSTEM GAS LOOP OPERATING WITH KRYPTON OVER A TURBINE INLET TEMPERATURE RANGE OF 1200° F TO 1600° F

by Alfred S. Valerino, Robert P. Macosko, Armen S. Asadourian, Thomas P. Hecker and Roman Kruchowy

Lewis Research Center
Cleveland, Ohio

NATIONAL AERONAUTICS AND SPACE ADMINISTRATION

ABSTRACT

Performance of a krypton gas power loop with a Brayton single-shaft rotating unit and heat-exchanger unit indicated an estimated loop net efficiency and gross alternator power output of approximately 30 percent and 12 kilowatts respectively at a turbine inlet temperature of 1600° F, a compressor discharge pressure of 37 psia and a compressor inlet temperature of 55° F. At a turbine inlet temperature of 1140° F, a compressor discharge pressure of 52 psia and a compressor inlet temperature of 100° F, the estimated net efficiency and gross alternator power were reduced to approximately 7 percent and 4 kilowatts respectively.

PRELIMINARY PERFORMANCE OF A BRAYTON-CYCLE-POWER-SYSTEM GAS LOOP OPERATING WITH KRYPTON OVER A TURBINE INLET TEMPERATURE RANGE OF 1200° F TO 1600° F

By Alfred S. Valerino, Robert P. Macosko, Armen S. Asadourian,

Thomas P. Hecker and Roman Kruchowy

Lewis Research Center

SUMMARY

The investigation of a krypton gas power loop incorporating a Brayton single-shaft rotating unit and a Brayton heat-exchanger unit was conducted at turbine inlet temperatures of 1200 to 1600° F at compressor discharge pressures of 15 to 56 psia and at compressor inlet temperatures of 70, 85 and 100° F. Limited data were obtained at the alternator high power levels because of a temperature limitation placed on the alternator internal temperatures. Isolated data points falling outside the parameter ranges were also obtained. Results of the investigation indicated an estimated loop net efficiency of approximately 30 percent at a turbine inlet temperature of 1600° F, a compressor discharge pressure of 37 psia and a compressor inlet temperature of 55° F. The gross alternator power output was approximately 12 kilowatts.

Increasing the compressor inlet temperature to 70° F, at a compressor discharge pressure of 35.5 psia, the estimated loop net efficiency and the gross alternator power output were approximately 29 percent and 9 kilowatts respectively. Recuperator effectiveness of 89 percent and 91 percent were obtained at the high and low pressure sides respectively for both of these conditions.

Decreasing the turbine inlet temperature resulted in significant reductions in the loop efficiency and alternator power output. At a temperature of 1140° F at the turbine inlet, a compressor discharge pressure of 52 psia and a compressor inlet temperature of 100° F, the estimated loop net efficiency dropped to approximately 7 percent; the gross alternator output to 4 kilowatts.

INTRODUCTION

NASA, since the advent of space exploration, has been engaged in the design and development of space electrical power generating systems. One such system currently under investigation operates on the Brayton thermodynamic cycle. Two configurations have been proposed, viz., a

two-shaft system producing 12 kilowatts of electrical power at 400 hertz with argon gas as the working fluid (ref. 1) and a single-shaft system designed to provide 2 to 15 kilowatts at 1200 hertz with a working gas mixture of helium and xenon having a molecular weight equivalent to that of krypton gas, 83.8 (refs. 2 and 3). Gas-lubricated bearings are employed to support the shafts of the turbomachinery of each configuration. Performance characteristics of the turbomachinery components of the two-shaft engine are reported in references 4 through 7.

The principal gas-loop components of the single-shaft system are the Brayton rotating unit (BRU---a turbine, alternator and compressor supported by a single shaft), the Brayton heat exchanger unit (BHXU---a single unit consisting of a gas-to-gas recuperator and a gas-to-liquid heat exchanger) and a heat source. Since the cost of the helium-xenon gas mixture is higher than krypton and because of the possibilities of leaks, the initial testing of the Brayton components and power loops reported herein was accomplished with krypton. Performance should improve when helium-xenon is the working gas due to its better heat-transfer characteristics. The performance of the BRU operating with argon and with krypton gases at a turbine inlet temperature of approximately 1500° F is reported in reference 8. The performance of a power system using an electric heat source, operating with krypton gas, in a vacuum environment, and at turbine inlet temperatures of 1250 to 1450° F is reported in reference 9.

In this investigation the performance of a krypton gas power loop having a Brayton single-shaft rotating unit and a Brayton heat exchanger unit in the gas loop was measured for turbine inlet temperatures from 1200 to 1600° F, compressor inlet temperatures of 70, 85 and 100° F and compressor discharge pressures of approximately 15 psia to 56 psia. The loop was operated for 210 hours in an atmospheric environment. The effects of compressor discharge pressure, turbine inlet temperature and compressor inlet temperature on compressor and turbine pressure ratios, alternator power output and system efficiencies obtained from the investigation are presented herein.

DESCRIPTION OF BRAYTON ROTATING UNIT AND HEAT EXCHANGER UNIT

The power loop tested, shown schematically in figure 1, consisted of a Brayton power conversion system and test support equipment.

The power conversion system consists of a rotating package (BRU) and a heat-exchanger unit (BHXU). These units were designed and fabricated by AiResearch Manufacturing Company.

Brayton Rotating Unit (BRU) - The BRU (fig. 2) which is 20 inches in diameter, 36 inches long and weighs approximately 145 pounds, consists of a turbine, an alternator and a compressor mounted on a single shaft designed to rotate at 36,000 rpm. The shaft is supported by gas-lubricated bearings designed to operate in the hydrodynamic (self-acting)

mode. The radial inflow turbine (ref. 10) has an impellor diameter of 4.97 inches. The radial outflow compressor impellor has a diameter of 4.25 inches. The four-pole brushless alternator is of the Lundell type having a solid rotor (3.3-inch diameter) and two stationary field windings for series and shunt excitation. The alternator is rated for 14.3 kilovolt-amperes at 0.75 lagging power factor, 120/208 volts, and a frequency of 1200 hertz. Cooling of the alternator is by means of two liquid passages (one redundant). Performance characteristics of the alternator are presented in references 11 and 12.

The BRU can be tested in either the vertical or horizontal position. For this test, the BRU is mounted vertically with the turbine end up in an aluminum framework.

Brayton Heat Exchanger Unit (BHXU). - The BHXU (fig. 3) incorporates a recuperator (gas-to-gas counterflow heat exchanger) with a waste heat (gas-to-liquid) cross-counterflow heat exchanger. The BHXU is 20 inches wide, 56 inches long and weighs approximately 440 pounds. The core of the recuperator (8.5 by 20 by 20 inches) consists of plate-and-fin sandwich construction brazed as a single unit. Two passages (one redundant) on the liquid side are provided. Core dimensions overall are 6.5 by 16 by 20 inches. The cores of both the recuperator and the waste heat exchanger were assembled into a single unit by welding to transition sections and headers.

A spool piece with a remotely controlled check valve is used to connect the outlet of the compressor to the inlet to the high-pressure side of the recuperator. Two ports, one on each side of the check valve, are employed to charge and vent the power conversion system of its working fluid (krypton).

DESCRIPTION OF TEST SUPPORT EQUIPMENT

The test support equipment includes an electric heat source, a gas-management module, a liquid-coolant or heat-rejection module, a gas-reclamation module, and an electrical subsystem.

Heat Source. - The electric heat source, located upstream of the turbine, uses Joule heating (I^2R heating) in a bank of 500 staggered Inconel-600 tubes (0.375-inch diameter by 0.065-inch wall thickness by 12 inches long) that are supported on each end by a ceramic header plate of 95-percent alumina. The ends of the tubes were connected with links in series to form three separate resistors. With a resistance of approximately 1½ ohms per resistor, and a delta connection to a 3-phase 208-volt line-to-line power source, approximately 90 kilowatts of electric power are available to heat the working gas. Gas flow is perpendicular to the staggered-tube bank. Photographs of the heater core and the assembled heater are presented in figures 4 and 5 respectively. The large tubes projecting from the heater (fig. 5) serve as instrumentation- and power-lead channels. The long extension from the heater body is required to

maintain low temperatures at the tube ends. The heat source and its insulated connections to the BHXU and the BRU are shown in figures 6 and 7 respectively. The insulation for the heat source and all other high-temperature surfaces was a high-silica fiber-type of blanket insulation. The insulation was effective for an operating temperature of 2000° F in air.

Gas-Management Module. - The gas-management module (fig. 8) consisted of pressurized working gas bottles, piping and valving required to charge and to vent the power conversion system as well as to supply jacking gas to the gas bearings (hydrostatic mode of operation) during loop startup and shutdown.

Two remotely controlled valves, parallel to one another, were employed to charge the loop, viz., a valve having a large flow discharge coefficient during the initial injection of the gas for startup, and a valve having a small flow discharge coefficient to add inventory when required during the testing. A calibrated orifice plate downstream of the paralleled valves was used to measure the injection rate during startup. Two remotely controlled valves parallel to one another were also employed to vent the gas from the loop; a high flow discharge coefficient valve for use during loop shutdown, and a small flow discharge coefficient valve for minor adjustment in inventory within the gas loop.

Gas-Reclamation Module. - The reclamation module consisted of two spherical vessels having a total volume of 100 cubic feet for receiving and storing the working gas during testing and shutdown. During the test, a pressure of approximately 8 psia was maintained in the vent tanks. A gas compressor was used to pump the gas from these vessels to gas inventory bottles to pressures of approximately 800 psig.

Heat Rejection Module. - (Fig. 9) - The liquid coolant used to remove waste heat from the power loop was a commercially available silicone-base fluid (Dow Corning-200, having a viscosity of 2 centistokes at 77° F). The coolant was pumped through one coolant passage of the BHXU to remove heat from the gas prior to its entrance to the compressor and through both coolant passages in the alternator. Coolant flow was required through both passages to maintain the acceptable alternator temperatures for the heat shield cone at the higher power levels and at turbine inlet temperatures above 1400° F. The poor conductivity of krypton compared to helium-xenon aggravated this problem. Flow through all of the coolant passages were remotely and independently controlled.

The heat transferred to the coolant from the BHXU and the alternator was removed by means of a coolant-to-water heat exchanger located upstream of and in series with a commercially available refrigeration unit (fig. 1).

All of the piping and valving from the refrigeration unit to the liquid coolant passages of the waste heat exchanger and to the

alternator, and their return lines to a common flow-through reservoir were insulated with a fibrous-silica aluminum-foil-backed type of insulating tape suitable for operation up to 900° F.

Electrical: - The alternator output is dissipated through a simulated vehicle load and a speed-controlled parasitic load. The simulated vehicle load is a commercially available adjustable and balanced three-phase resistive load bank. A breadboard version of the Brayton engine speed controller was used. The operating principle of the engine speed controller is discussed in reference 13. The speed control consists of three separate electronic speed controllers and three three-phase parasitic loads. The speed controller applies parasitic load as shaft speed increases above 36,000 rpm and maintains it to within 2 percent of nominal.

INSTRUMENTATION

The instrumentation used for this test consisted of pressure transducers, thermocouples, a flow venturi, turbine flowmeters, speed sensors and power monitoring equipment.

Absolute Pressures. - A static pressure tap with a strain-gage type of transducer was employed at the inlet and outlet of each of the compressor and turbine, and at the inlet to the flow venturi located between the outlet of the high-pressure side of the recuperator and the inlet to the heat source.

Differential Pressures. - Static taps and differential strain-gage transducers were used to obtain the pressure drop across the low-pressure side of the recuperator, across the high-pressure side of the recuperator, across the liquid side of the waste heat exchanger, and across the engine venturi inlet to throat sections.

Temperatures. - Gas temperatures at the inlet and outlet of the turbine were each obtained from the average of 3 chromel-alumel thermocouple rake. Gas temperatures at the inlet and outlet of the recuperator high pressure side and the inlet to the recuperator low pressure side were obtained from an average of four chromel-alumel probe-type thermocouples. The gas temperature at the outlet of the recuperator low pressure side was obtained from an average of 10 chromel-alumel probe-type thermocouples. The gas temperature at the outlet of the gas side of the waste heat exchanger was obtained from the average of four chromel-alumel probe-type thermocouples. Liquid coolant temperatures into and out of the waste heat exchanger were each obtained from an iron-constantan skin thermocouple.

Flow Rates: - System gas flow rates were calculated from the engine venturi inlet pressure, venturi differential pressure and the temperature at the outlet of the high pressure side of the recuperator.

Liquid coolant flow rates to the waste heat exchanger of the BHXU and to both alternator passages were individually sensed by turbine-type flowmeters. Signals from these flowmeters were conditioned to dc outputs using frequency-to-dc voltage converters.

BRU Shaft Speed. - Rotative speed was obtained by means of both alternator frequency and a capacitance probe located in the BRU near the compressor journal bearing. The signal from the probe was conditioned to a dc output using a frequency-to-dc voltage converter. Speed was observed on a frequency counter.

Electrical. - The power, voltage and current of each of the three phases of the alternator and the simulated vehicle load were measured with true root-mean-square instruments.

Instrumentation output signals were displayed in the control room and transmitted to a dedicated on-line digital computer. The digital computer has 200 input channels and converted the required data to engineering units for display by an electric typewriter.

PROCEDURE

The gas loop startup and shutdown techniques were similar to those described in reference 11. During the 210-hour test, constant values of compressor inlet and turbine inlet temperatures were maintained while compressor discharge pressure was varied. Compressor inlet temperatures were measured at the outlet of the gas side of the waste heat exchanger.

The investigation was conducted through a turbine inlet temperature range of 1200° F to 1600° F and compressor discharge pressure range of 15 psia to 56 psia at compressor inlet temperatures of 55, 70, 85 and 100° F. Isolated data points falling outside these ranges were also taken.

Two limitations were set during the test, viz., (1) to obtain data at a minimum alternator power output of approximately 2 kilowatts and (2) to minimize the amount of test time with alternator internal temperature exceeding 450° F. Because of these limitations, the amount of data taken at some of the turbine inlet temperatures was limited. It is expected, because of the much better heat-transfer properties of the proposed Brayton engine working fluid, that the high alternator internal temperatures will not be as limiting a factor when the system is operated with the helium-xenon gas mixture.

Data were obtained at an alternator frequency of approximately 1220 hertz (rotative speed of 36,600 rpm) instead of 1200 hertz due to

a mistuning of the speed controller. The speed controller was later tuned to obtain the proper operating frequency.

DISCUSSION

Performance characteristics of the krypton gas power loop, herein designated as power system, and its components are presented for a nominal rotative speed of 36,600 rpm (1220 hertz).

Brayton Rotating Unit, BRU

The effects of the compressor discharge pressure P_{CD} on the compressor static pressure ratio (P_{CD}/P_{CI}) on the engine flowrate W and on the turbine static pressure ratio (P_{TI}/P_{TD}) at nominal compressor inlet temperatures T_{CI} of 70, 85, and 100° F are shown in figures 10(a) through 10(e) for turbine inlet temperatures from 1200 to 1600° F.

Engine flowrate. - The engine flowrate is determined by the operating conditions at the compressor. Weight flow increased with increasing compressor discharge pressure, P_{CD}, and with decreasing compressor inlet temperature, T_{CI}, as demonstrated in figures 10(a), 10(b), and 10(e). The maximum flowrate of approximately 1.67 pounds per second obtained during the testing was at a compressor discharge pressure of 56 psia at a compressor inlet temperature of 100° F.

Compressor and turbine static pressure ratios. - The compressor pressure ratio (discharge to inlet, P_{CD}/P_{CI}) decreased with increasing P_{CD} and with increasing T_{CI}. Effects due to T_{CI} on P_{CD}/P_{CI} were more significant at a turbine inlet temperature of 1600° F (fig. 10(e)) and at a P_{CD} of 40 psia the compressor pressure ratio was reduced approximately from 2 to 1.88 by increasing T_{CI} from 55 to 100° F.

The turbine pressure ratio (inlet to discharge, P_{TI}/P_{TD}) increased slightly with increasing compressor discharge pressure P_{CD}. However, increasing compressor inlet temperature T_{CI} resulted in decreasing the turbine pressure ratio. At T_{TI} of 1600° F (fig. 10(e)) at P_{CD} = 40 psia, increasing T_{TI} from 55 to 100° F, resulted in a reduction in P_{TI}/P_{TD} from approximately 1.86 to approximately 1.73.

Crossplots to demonstrate the turbine inlet temperature, T_{TI}, effects on the compressor and turbine pressure ratios are presented in figures 11 and 12 respectively. Decreases in both P_{CD}/P_{CI} and P_{TI}/P_{TD} resulted as T_{TI} was increased. At a compressor inlet temperature of 100° F and at P_{CD} of approximately 50 psia, P_{CD}/P_{CI} was decreased from approximately 1.87 to 1.82 and P_{TD}/P_{TI} from approximately 1.75 to 1.71 when T_{TI} was decreased from 1600 to 1140° F.

Alternator power. - The effects of the test variables on the alternator power output are shown in figure 13. Increases in power output were obtained with increasing compressor discharge pressure, with increasing turbine inlet temperature and with decreasing compressor inlet temperature. Increasing P_{CD} from 15 psia to 48 psia at $T_{TI} = 1600^{\circ}$ F and $T_{CI} = 100^{\circ}$ F increased alternator power output from 3 kW to approximately 12 kW (fig. 13(c)). At a P_{CD} of 52 psia (fig. 13(c)) the alternator power of approximately 4 kW was obtained by decreasing the turbine inlet temperature to 1140° F. At a P_{CD} of 37 psia and a turbine inlet temperature of 1600° F, decreasing the compressor inlet temperature from 100 to 55° F caused an increase in alternator output from approximately 9.2 kW to approximately 12 kW; an increase in power of approximately 29 percent. At $T_{TI} = 1500^{\circ}$ F and $P_{CD} = 39$ psia the alternator output was increased approximately 41 percent (8.2 to 11.6 kW) when T_{CI} was reduced from 100 to 55° F.

Brayton Heat Exchanger Unit

Recuperator. - The variation of the recuperator temperature effectiveness and pressure drop with compressor discharge pressure at a turbine inlet temperature of 1600° F are presented in figure 14. The temperature effectiveness of the low pressure side of the recuperator, E_{TL}, (turbine discharge to waste heat-heat exchanger inlet) is defined as:

$$E_{TL} = \frac{T_1 - T_2}{T_1 - T_3} \qquad \text{where}$$

T_1 = gas temperature at inlet of recuperator low pressure side

T_2 = gas temperature at outlet of recuperator low pressure side

T_3 = gas temperature at inlet of recuperator high pressure side

The temperature effectiveness of the recuperator high pressure side, E_{TH}, is defined as

$$E_{TH} = \frac{(T_4 - T_3)}{(T_1 - T_3)} \qquad \text{where}$$

T_4 = gas temperature at the outlet of the recuperator high pressure side

The data presented in figure 14 indicate that the compressor inlet temperature, T_{CI}, has no significant influence on either the temperature effectiveness or the pressure drops. On the low pressure side, E_{TL} was reduced from approximately 95 percent to 92 percent and the pressure drop, ΔP_L, was increased from approximately ¼ psid to approximately 1/3 psid when the compressor discharge pressure was increased from 15 to 36 psia. At the high alternator power condition, $T_{CI} = 55^{\circ}$ F at $T_{TI} = 1600^{\circ}$ F, an E_{TL} of approximately 91½ percent was obtained. On the high pressure side, E_{TH} was essentially constant at approximately 89½ percent with increasing P_{CD}. The pressure drop, ΔP_H, increased from approximately 1/3 psid to 1/2 psid.

Waste heat exchanger. - The variation of the temperature effectiveness of the gas side of the waste heat exchanger, E_{TG}, with compressor discharge pressure is presented in figure 15. The effectiveness E_{TG} is defined as

$$E_{TG} = \frac{(T_2-T_5)}{(T_2-T_6)} \qquad \text{where}$$

T_5 = gas temperature at the gas outlet side of the waste heat exchanger

T_6 = liquid coolant temperature at the liquid inlet side of the waste heat exchanger

The effectiveness, E_{TG}, decreased with increasing compressor discharge pressure. The significant effect, however, is due to changes to the compressor inlet temperature at $T_{CI} = 70^{\circ}$ F. E_{TG} was reduced from 96 percent to 95 percent as the compressor discharge pressure P_{CD} was increased from approximately 15.5 psia to 29 psia. Increasing compressor inlet temperature to 100° F resulted in a reduction of approximately 9 percentage points over the same P_{CD} range.

The temperature effectiveness of the liquid coolant side of the wasteheat exchanger, E_{TC}, is presented in figure 16 as a function of liquid flowrates at five different combinations of liquid temperatures at the heat exchanger inlet and gas temperature at the compressor inlet. The effectiveness of the liquid side is defined as

$$E_{TC} = \frac{T_7-T_6}{T_2-T_6} \qquad \text{where}$$

T_7 = liquid coolant temperature at outlet side of the waste heat exchanger

Increasing liquid flowrate resulted in relatively small reductions in the effectiveness. E_{TC} was significantly influenced by both the gas temperature to the compressor and the liquid coolant inlet temperature, indicating that the gas side controlled the heat transfer. Effectiveness values above 90 percent were obtained at the combination of high compressor inlet and low liquid inlet temperatures (100 and 45° F respectively). Lower E_{TC} resulted when the compressor inlet temperature was reduced and/or the liquid inlet temperature was increased. Values of effectiveness below 70 percent were obtained when the compressor inlet temperature was 70° F with the liquid inlet temperature at 60° F.

The variation of liquid side pressure drop, ΔP_C with liquid flowrate, and gas temperature at the compressor inlet is demonstrated in figure 17. Increases in the pressure drop were obtained with increases in liquid flowrate and with decreasing compressor inlet gas temperature. At a liquid flowrate of 1.5 gallons per minute, the ΔP_C increased from 2.5 psid to 3.85 psid by reducing the gas temperature to the compressor from 100 to 70° F, at 1.8 gallons per minute from approximately 3.1 psid to 4.8 psid.

Efficiency. - The effects of compressor discharge pressure on system efficiency are presented in figure 19. Gross system efficiency, η_{SG} is derived from the ratio of gross alternator power output to the heater thermal input to the krypton gas.

$$\eta_{SG} = \frac{A_p}{WC_p(T_{TI}-T_4)K} \qquad \text{where}$$

A_p = gross alternator power output

W = engine flowrate

C_p = specific heat at constant gas pressure

T_{TI} = turbine inlet temperature

T_4 = temperature at outlet of high pressure side of the recuperator

K = conversion factor (BTU to kW)

If the power required to operate all the auxiliaries of a flight version Brayton Cycle Power System at the minimum speed control, is assumed to be 1400 watts as is done in reference 9, then a system net efficiency, η_{SN} can be estimated. System gross efficiencies for the test parameters and the estimated net efficiencies at turbine inlet temperatures of 1600, 1200 and 1140° F only are presented in figure 19.

At a P_{CD} of 37 psia and a compressor inlet temperature of 55° F a gross efficiency of approximately 34 percent resulted; estimated net efficiency was approximately 30 percent.

Increasing the compressor inlet temperature to 70° F at a compressor discharge pressure of approximately 35.5 psia the gross and estimated net efficiencies decreased to approximately 33 percent and 29 percent respectively.

At a compressor inlet temperature of 100° F (fig. 19(c)) at T_{TI} = 1600° F and P_{CD} = 48 psia, the gross and estimated net efficiencies were approximately 30 percent and 27 percent respectively. Decreasing turbine inlet temperature to 1140° F resulted in an estimated net efficiency at P_{CD} = 52 psia of approximately 7 percent; a gross efficiency of approximately 11 percent.

CONCLUDING REMARKS

The performance characteristics of a krypton gas power loop with a Brayton single-shaft rotating unit and a Brayton heat-exchanger unit were obtained through a range of compressor inlet temperatures, turbine inlet temperatures and compressor discharge pressures. Krypton has the same molecular weight as the helium-xenon mixture planned for use in the Brayton power system.

Results of the investigation include:

(1) Assuming a 1400-watt power load to operate auxiliaries, an estimated system net efficiency of approximately 30 percent was obtained at a turbine inlet temperature of 1600° F, a compressor discharge pressure of 37 psia and at a compressor inlet temperature of 55° F. The resulting recuperator temperature effectiveness on the high and low pressure sides were approximately 89 percent and 91 percent respectively. The gross alternator power output corresponding to these operating conditions was approximately 12 kW.

(2) At a turbine inlet temperature of 1140° F a compressor discharge pressure of 52 psia and at a compressor inlet temperature of 100° F, an estimated net efficiency of approximately 7 percent resulted. At these conditions the gross alternator output was approximately 4 kW.

Lewis Research Center
National Aeronautics and Space Administration
Cleveland, Ohio, February 25, 1970

REFERENCES

1. Bernatowicz, Daniel T.: NASA Solar Brayton Cycle Studies. Paper presented at the Symposium on Solar Dynamics Systems, Interagency Advanced Power Group, Washington, D.C., Sept. 24-25, 1963.

2. Klann, John L.: 2 to 10 Kilowatt Solar or Radioisotope Brayton Power System. Intersociety Energy Conversion Engineering Conference. Vol. 1. IEEE, 1968, pp. 407-415.

3. Klann, John L.: Analysis and Selection of Design Conditions for a Radioisotope Brayton-Cycle Space Powerplant. NASA TN D-4600, 1968.

4. Wong, Robert Y.; Evans, Robert C.; and Spackman, Donald J.: Preliminary Experimental Evaluation of a Brayton Cycle Turbocompressor Operating on Gas Bearings. NASA TM X-52261, 1966.

5. Wood, James C.; Valgora, Martin E.; and Tryon, H. B.: Hot Performance Characteristics of a Gas Bearing Brayton Cycle Turboalternator. Proceedings of the 4th Intersociety Energy Conversion Engineering Conference. AIChE, 1969, pp. 659-667.

6. Kruchowy, Roman; Wood, James C.; and Curreri, Joseph S.: Performance of a Turboalternator Gas-Bearing System at Steady-State Conditions. NASA TN D-5542, 1969.

7. Curreri, Joseph S.; Kruchowy, Roman; and Wood, James C.: Turbine Performance in a Gas-Bearing Brayton Cycle Turboalternator. NASA TN D-5604, 1969.

8. Wong, Robert Y.; Klassen, Hugh A.; Evans, Robert C.; and Winzig, Charles H.: Preliminary Investigation of a Single-Shaft Brayton Rotating Unit Designed for a 2 to 10-Kilowatt Space Power Generation System. NASA TM X-1869, 1969.

9. Fenn, David B.; Deyo, James N.; Miller, Thomas J.; and Vernon, Richard W.: Experimental Performance of a 2-15 Kilowatt Brayton Power System in the Space Power Facility Using Krypton. NASA TM X-52750, 1970.

10. Nusbaum, William J.; and Kofskey, Milton G.: Cold Performance Evaluation of a 4.97-Inch Radial-Inflow Turbine Design for Single-Shaft Brayton Cycle Space-Power Systems. NASA TN D-5090, 1969.

11. Repas, David S.; and Edkin, Richard A.: Performance Characteristics of a 14.3-Kilovolt-Ampere Modified Lundell Alternator for 1200 Hertz Brayton Cycle Space-Power System. NASA TN D-5405, 1969.

12. Bollenbacher, Gary; and Wimmer, Heinz L.: Electromagnetic Performance Limits of a 1200-Hertz Lundell Alternator for a Brayton-Cycle Power System. NASA TM X-52742, 1969.

13. Perz, Dennis A.; and Valgora, Martin E.: Experimental Evaluation of Volt-Ampere Loading and Output Distortion for a Turboalternator With Multiple Load Phase-Controlled Parasitic Speed Controller. NASA TN D-5603, 1969.

14. Cantoni, Dennis A.; and Thomas, Ronald L.: Analog Computer Studies of a 2 to 10 Kilowatts Electric Brayton Cycle Space Power System Including Startup and Shutdown. Proceedings of the 4th Intersociety Energy Conversion Engineering Conference. AIChE, 1969, pp. 668-678.

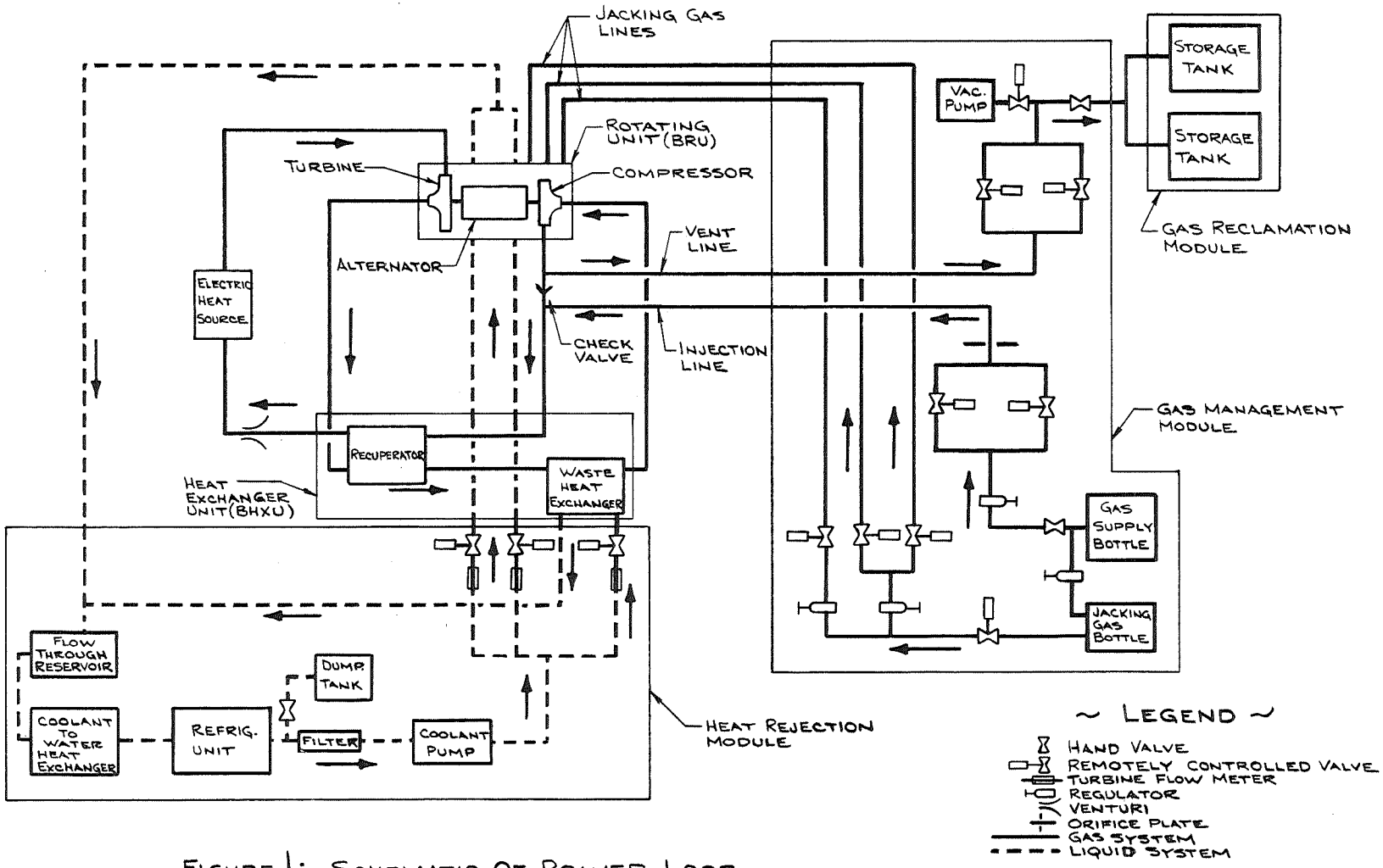

FIGURE 1: SCHEMATIC OF POWER LOOP

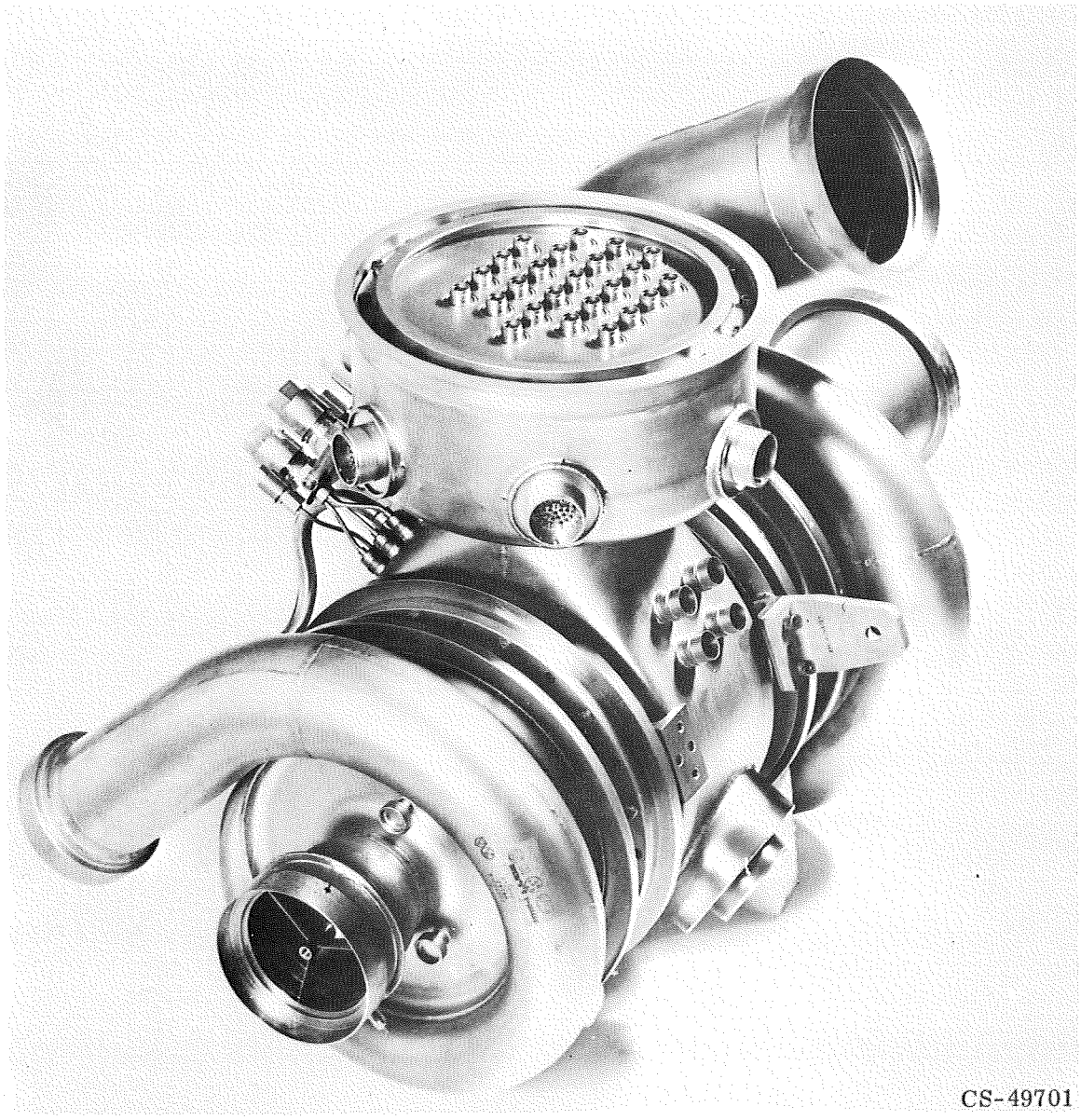

Figure 2: Brayton Rotating Unit.

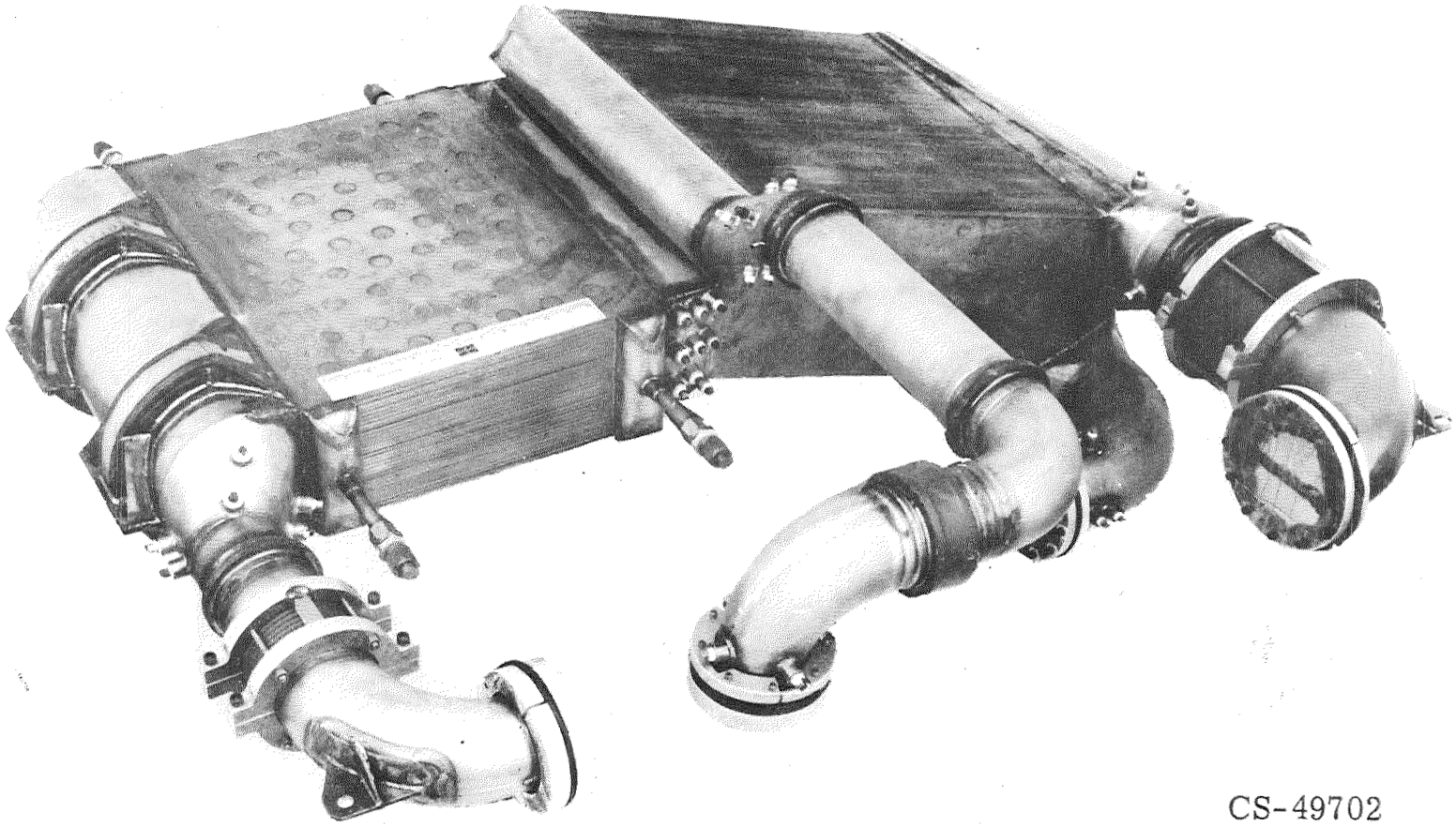

Figure 3: Brayton Heat Exchanger Unit.

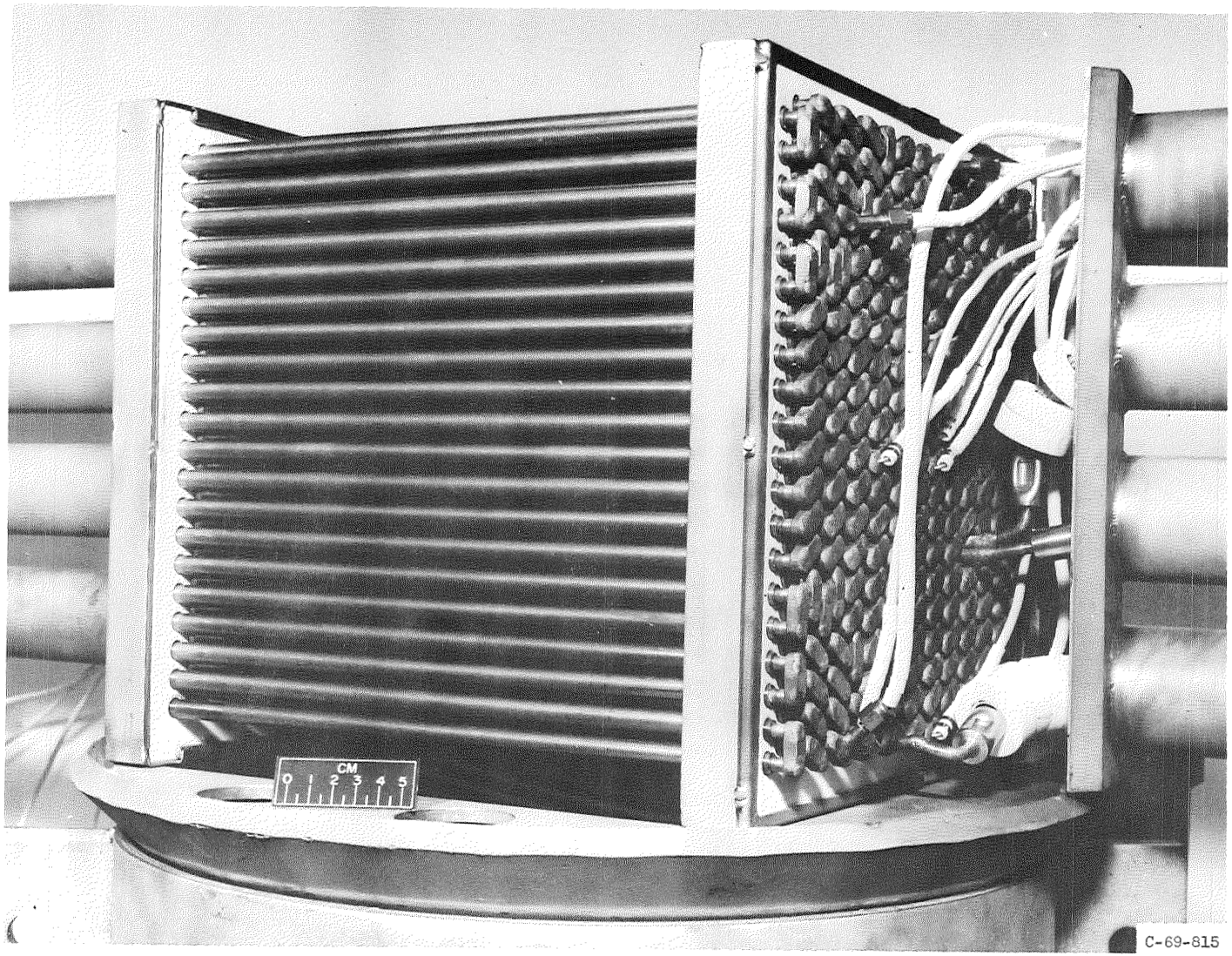

Figure 4: Core bundle of the electric heat source.

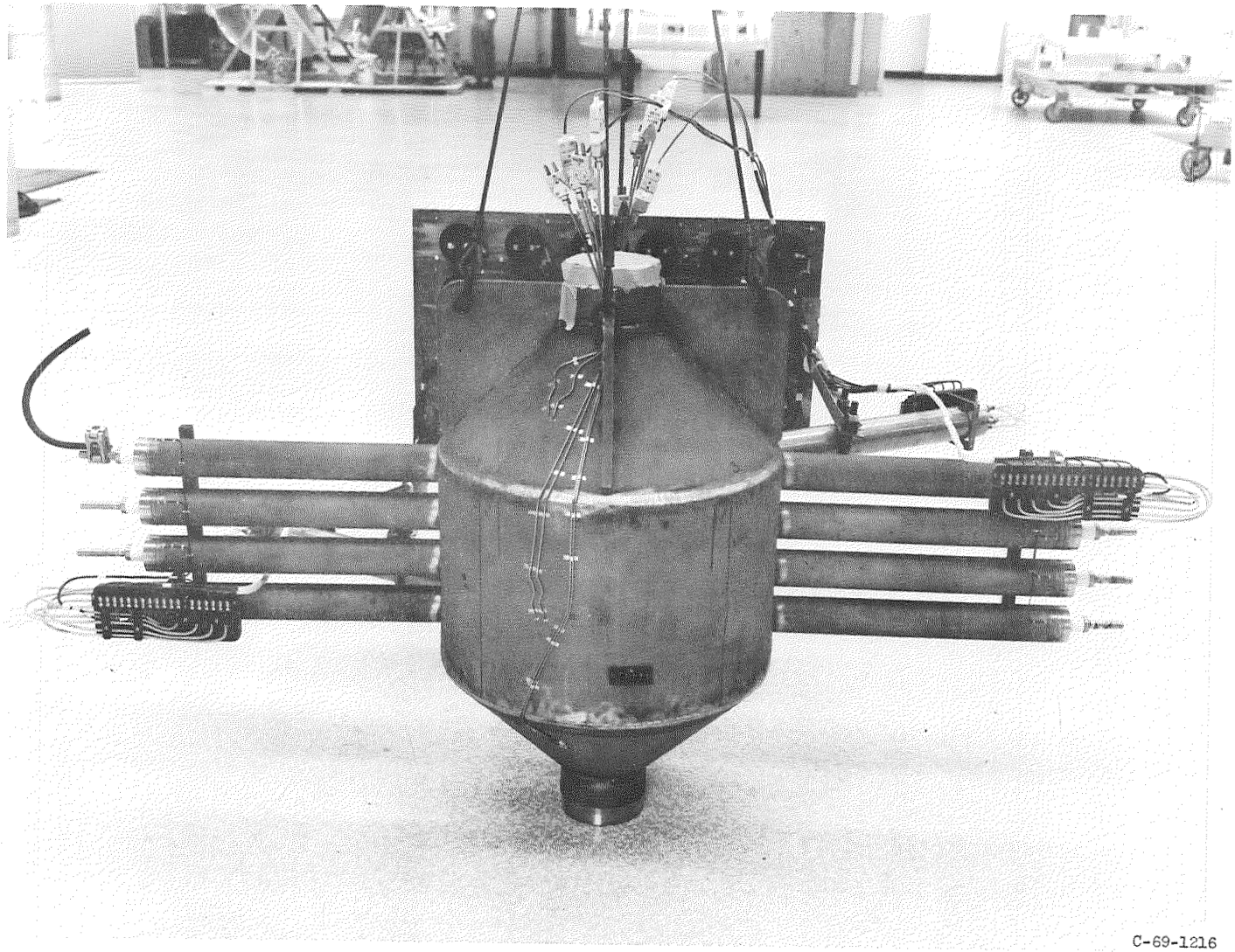

C-69-1216

Figure 5: Assembled heat source.

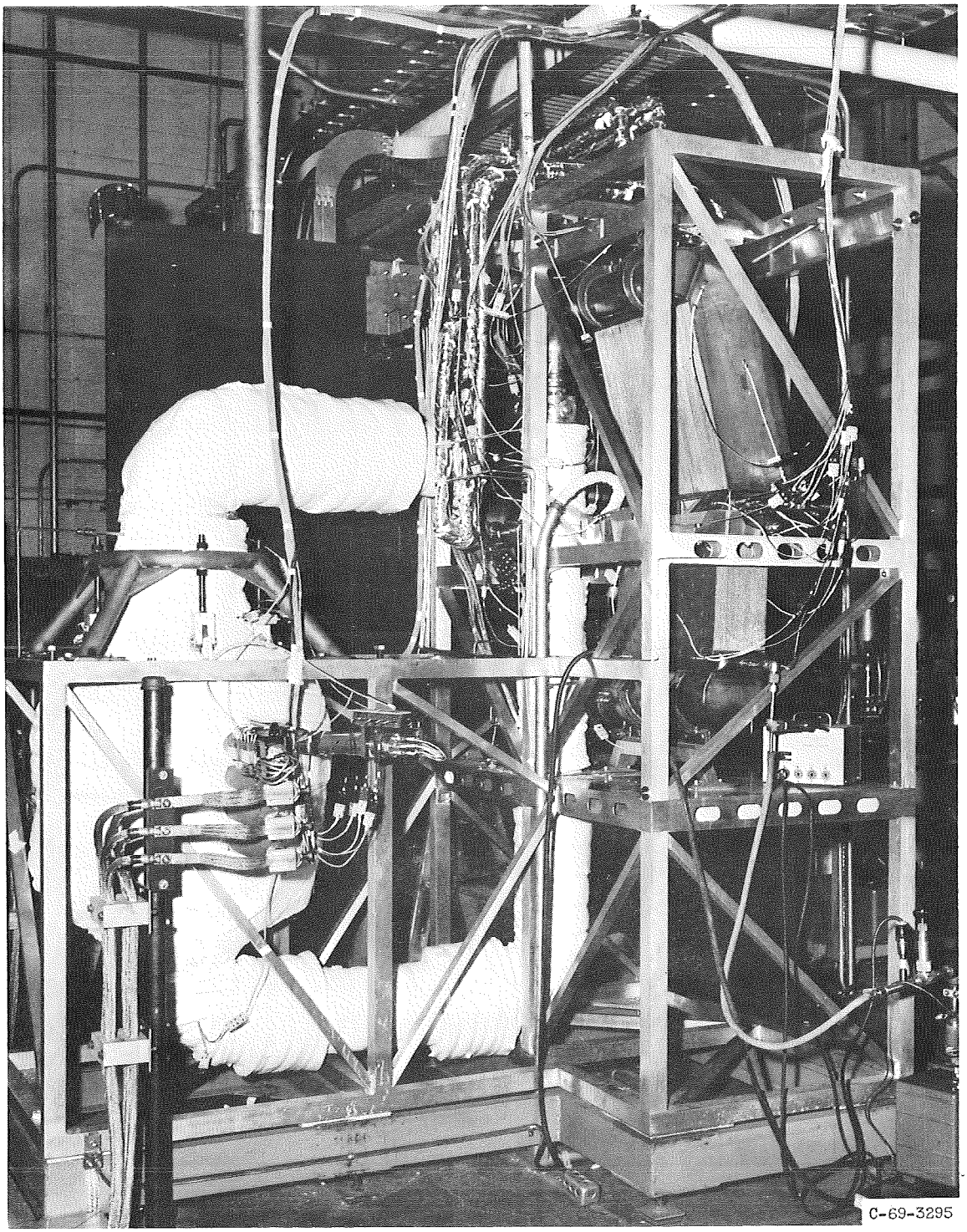

Figure 6: Electric heat source and Brayton Heat Exchanger Unit installation.

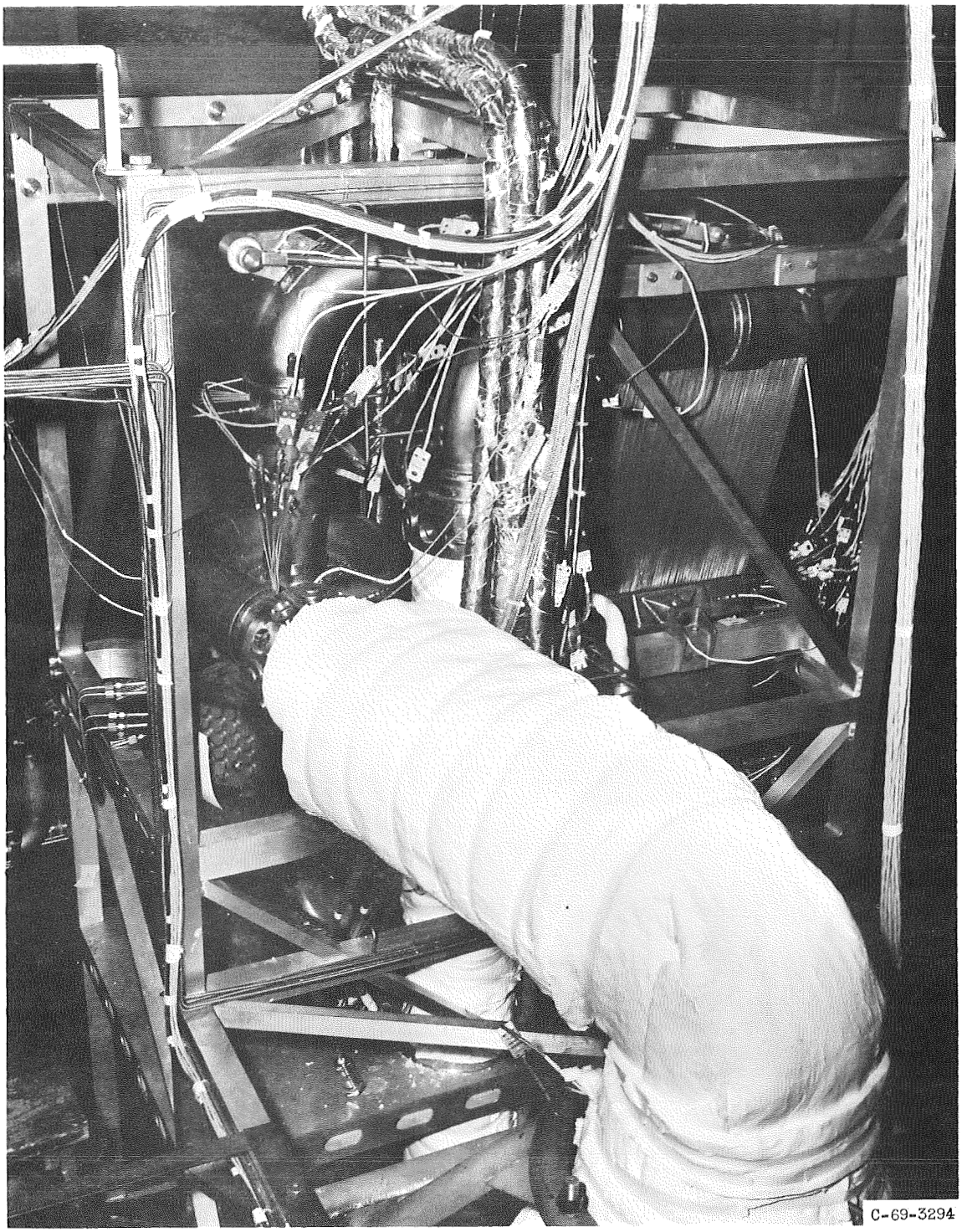

Figure 7: Electric heat source and Brayton rotating unit installation.

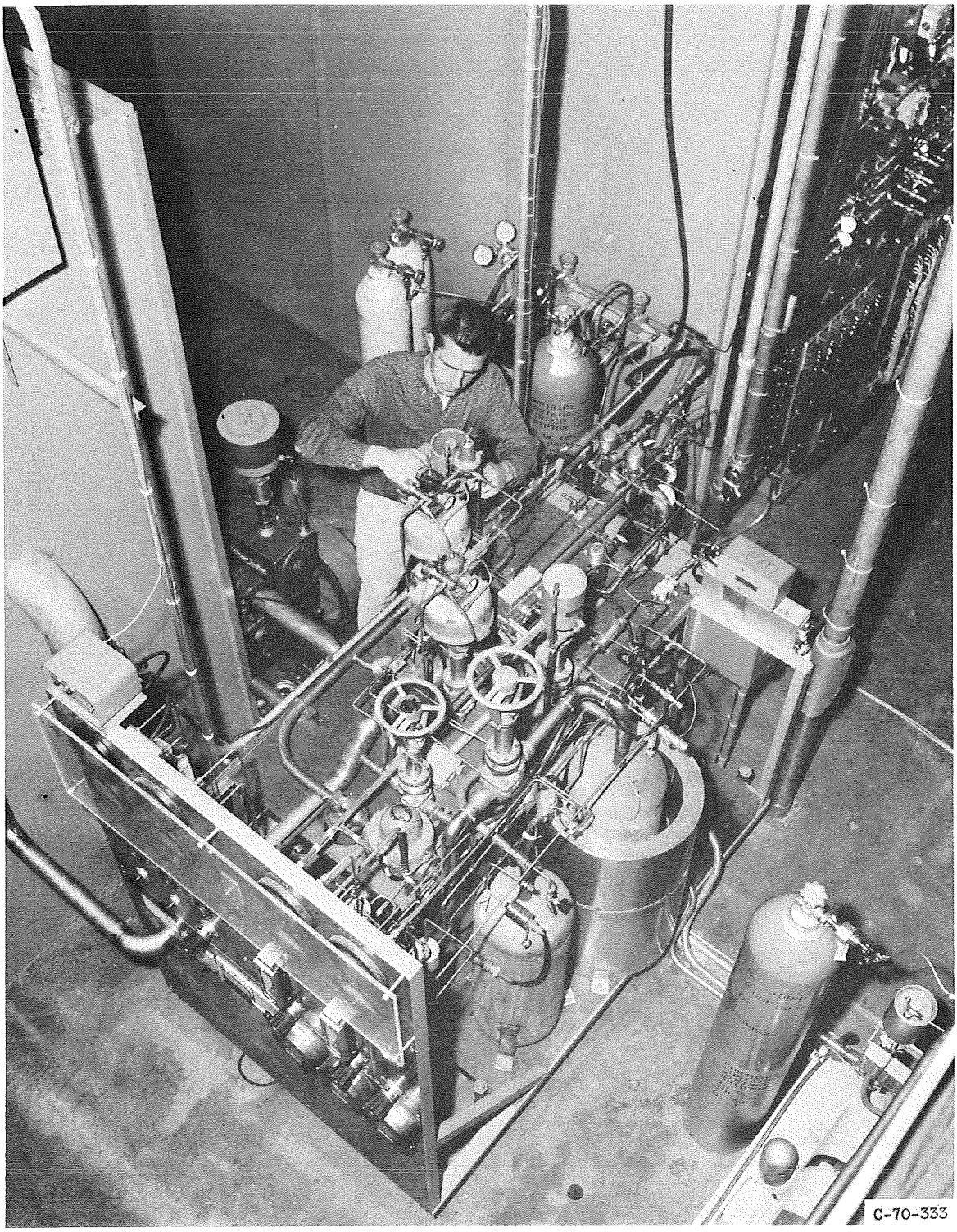

Figure 8: Gas management module.

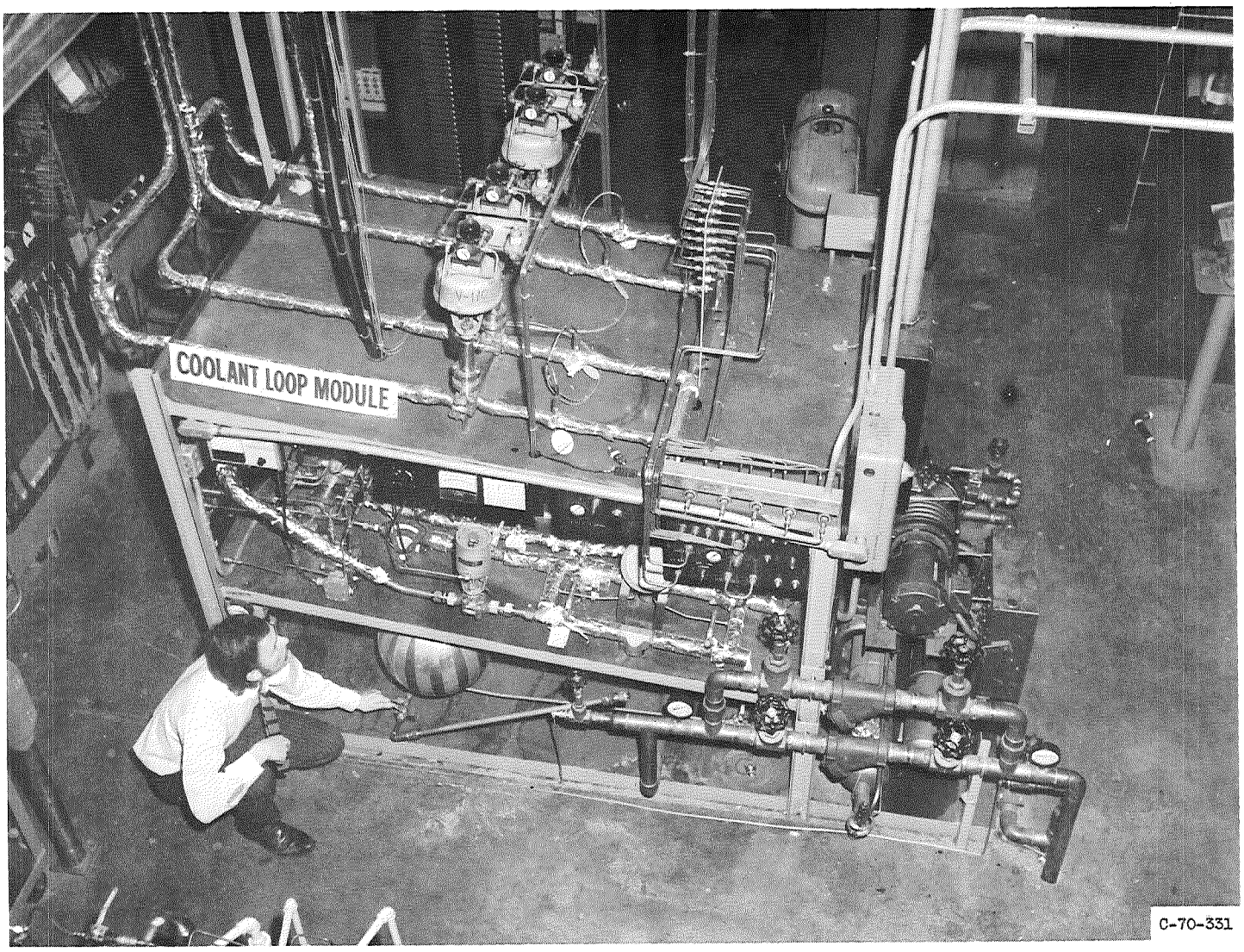

Figure 9: Heat rejection module.

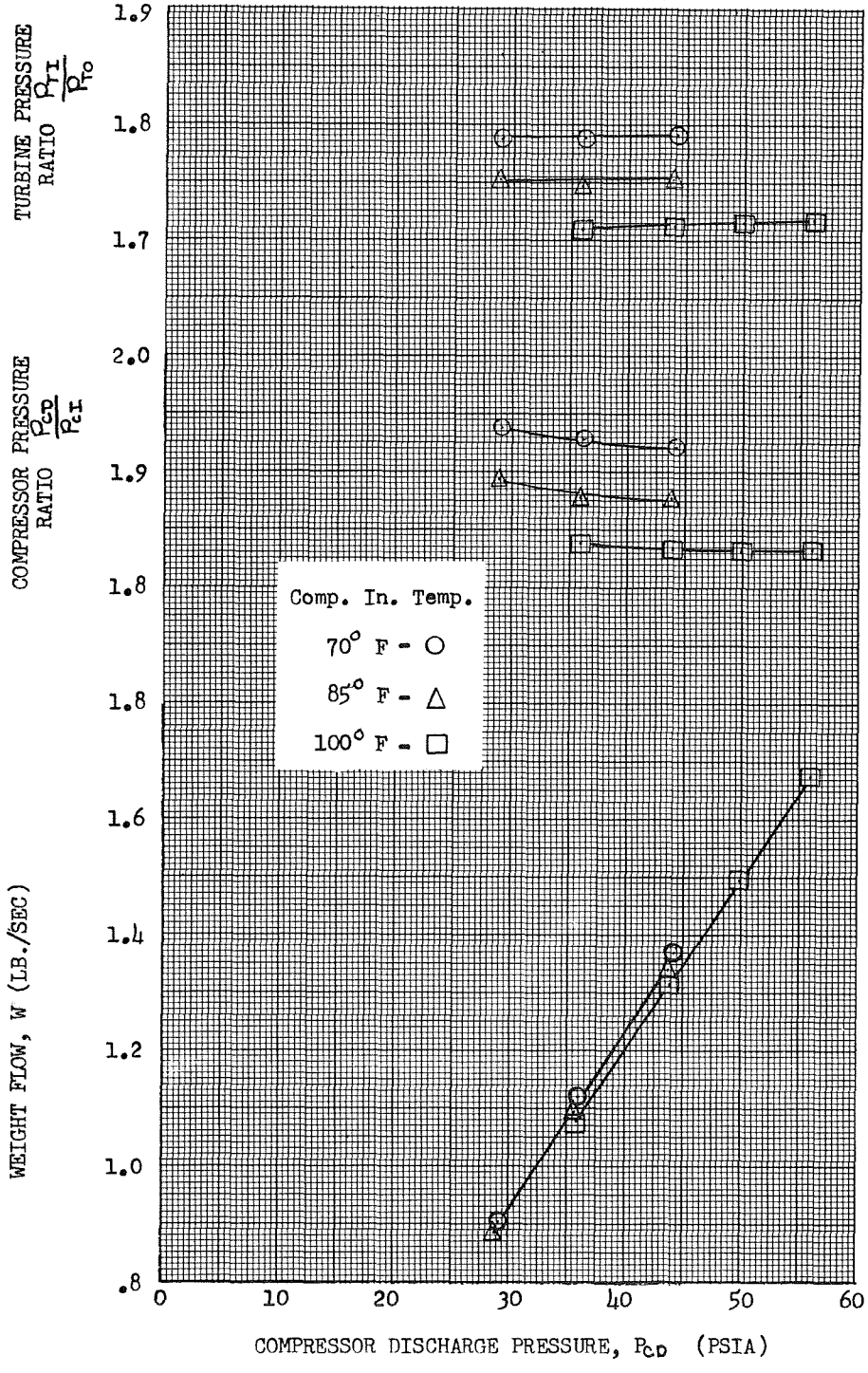

Figure 10: Effect of Compressor Discharge Pressure on Turbine Pressure Ratio, Compressor Pressure Ratio, and Weight Flow. Krypton Gas
(a) Turbine Inlet Temperature 1200° F.

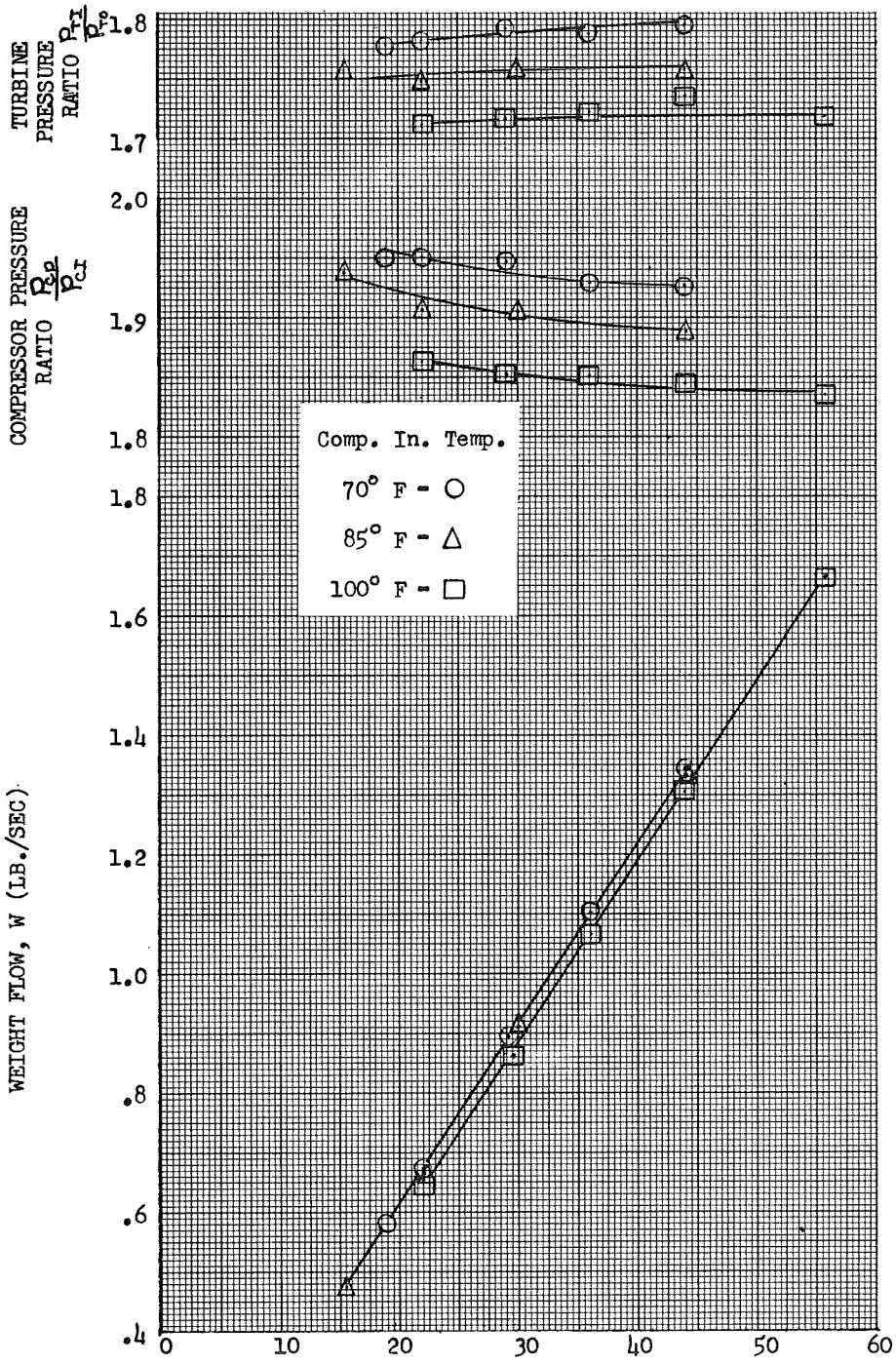

Figure 10: Effect of Compressor Discharge Pressure on Turbine Pressure Ratio, Compressor Pressure Ratio, and Weight Flow, Krypton Gas
(b) Turbine Inlet Temperature 1300° F.

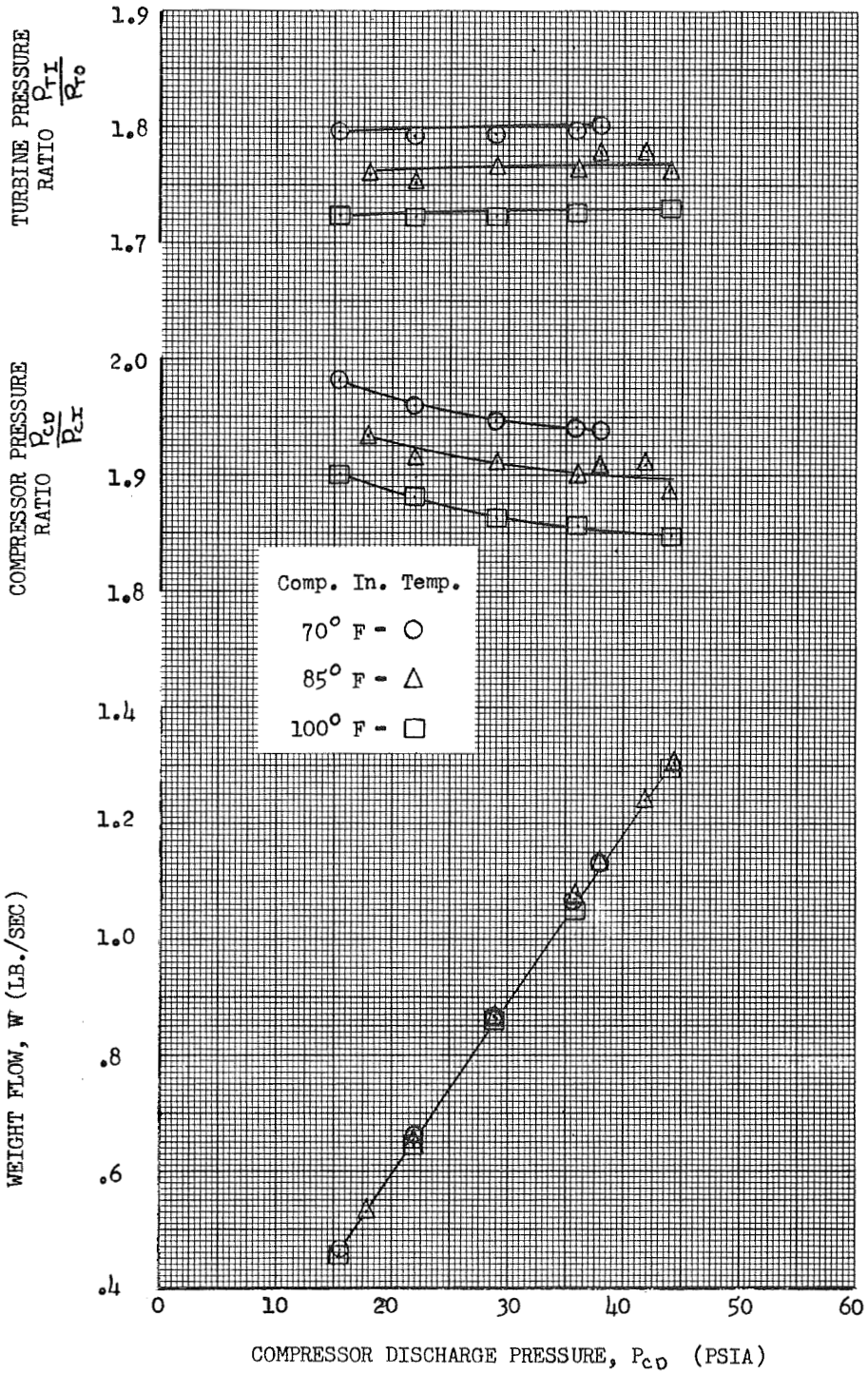

Figure 10: Effect of Compressor Discharge Pressure on Turbine Pressure Ratio, Compressor Pressure Ratio, and Weight Flow. Krypton Gas (c) Turbine Inlet Temperature 1400° F.

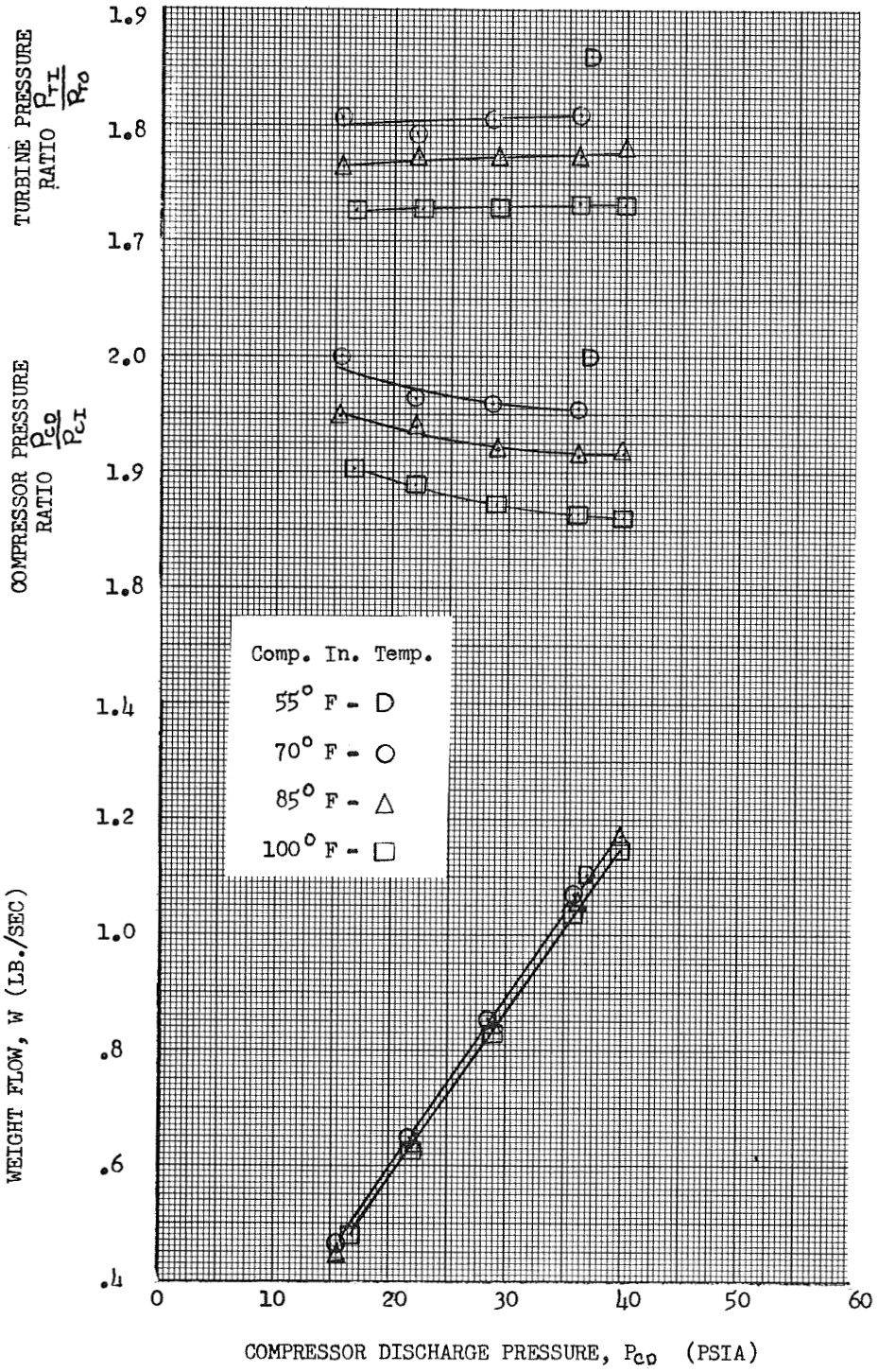

Figure 10: Effect of Compressor Discharge Pressure on Turbine Pressure Ratio, Compressor Pressure Ratio, and Weight Flow.
(d) Turbine Inlet Temperature 1500° F. Krypton Gas

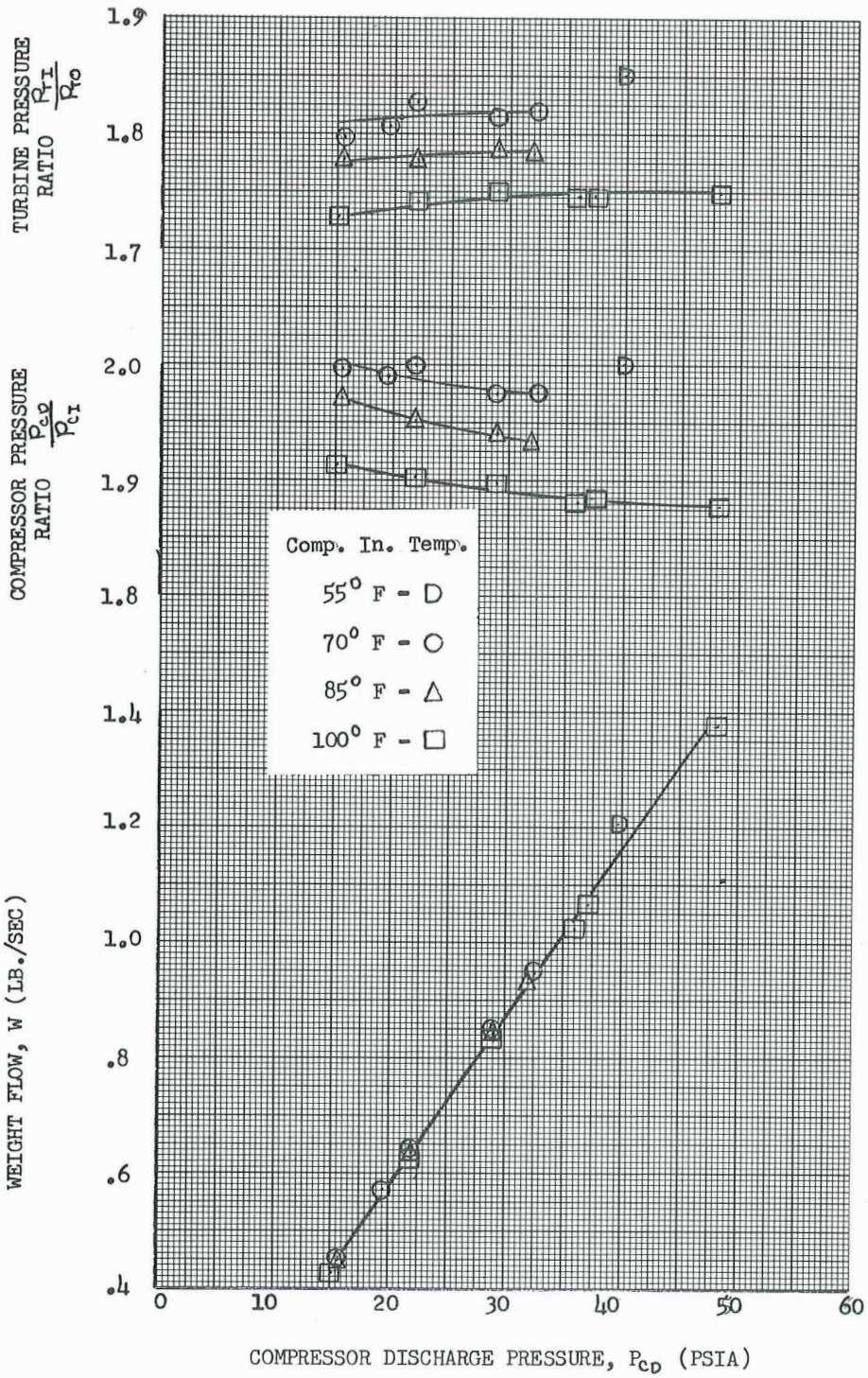

Figure 10: Effect of Compressor Discharge Pressure on Turbine Pressure Ratio, Compressor Pressure Ratio, and Weight Flow. Krypton Gas
(e) Turbine Inlet Temperature 1600° F.

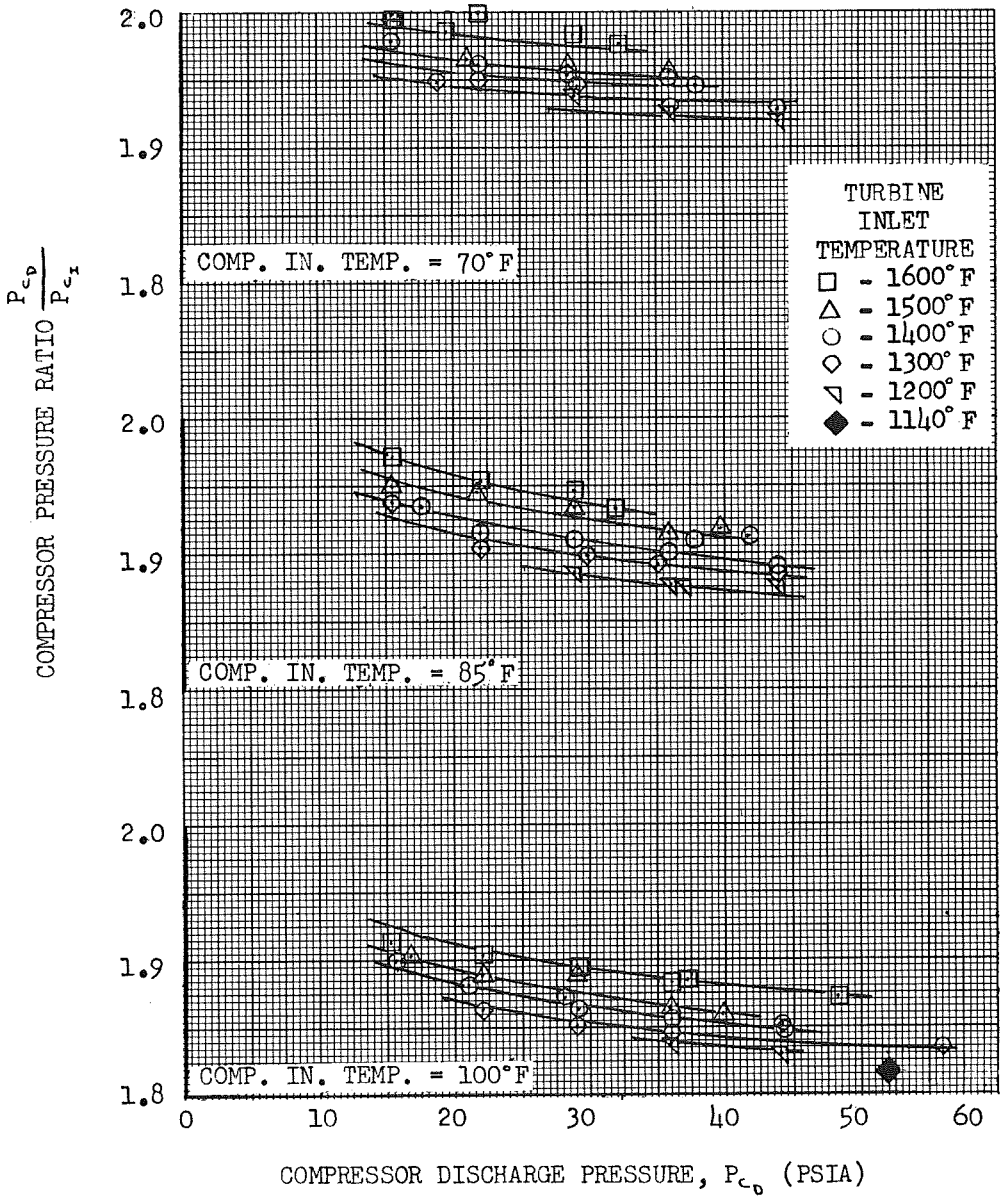

Figure 11: Effect of Compressor Discharge pressure on Compressor pressure ratio. Krypton Gas

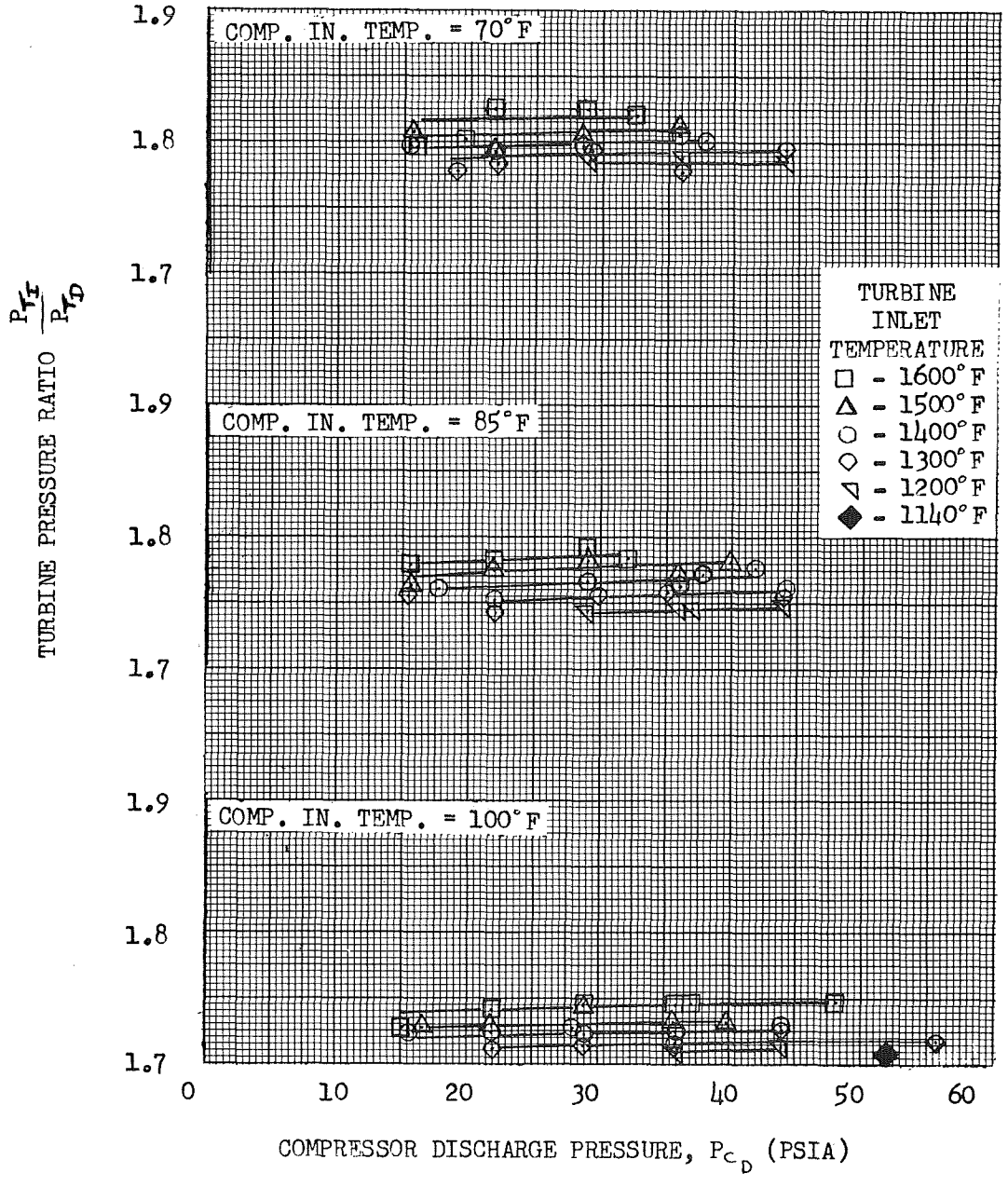

Figure 12: Effect of Compressor Discharge pressure on Turbine pressure ratio. Krypton Gas

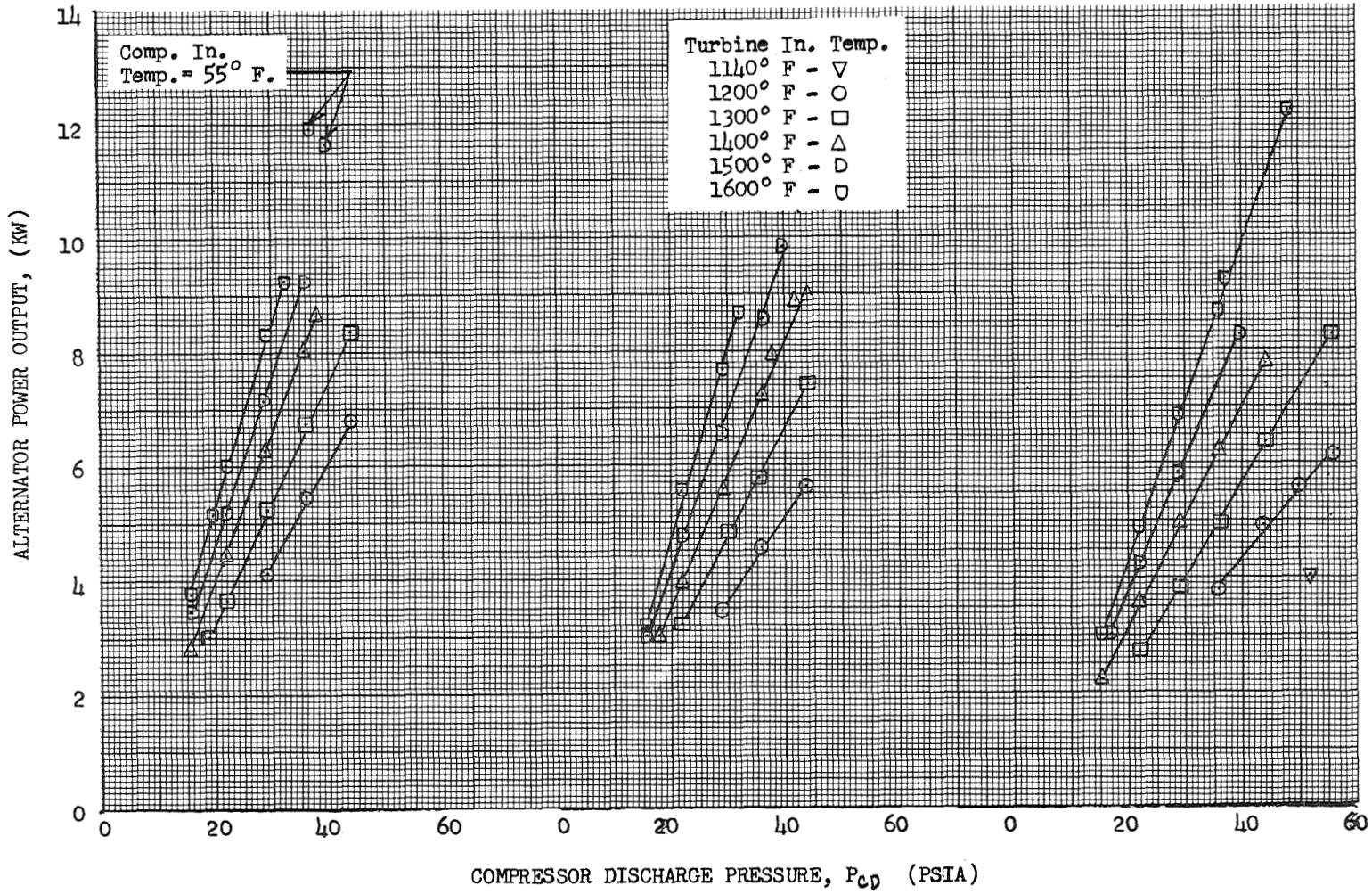

Figure 13: Effect of Compressor Discharge Pressure on Alternator Power Output. Krypton Gas

(a) Compressor Inlet Temperature = 70° F.

(b) Compressor Inlet Temperature = 85° F.

(c) Compressor Inlet Temperature = 100° F.

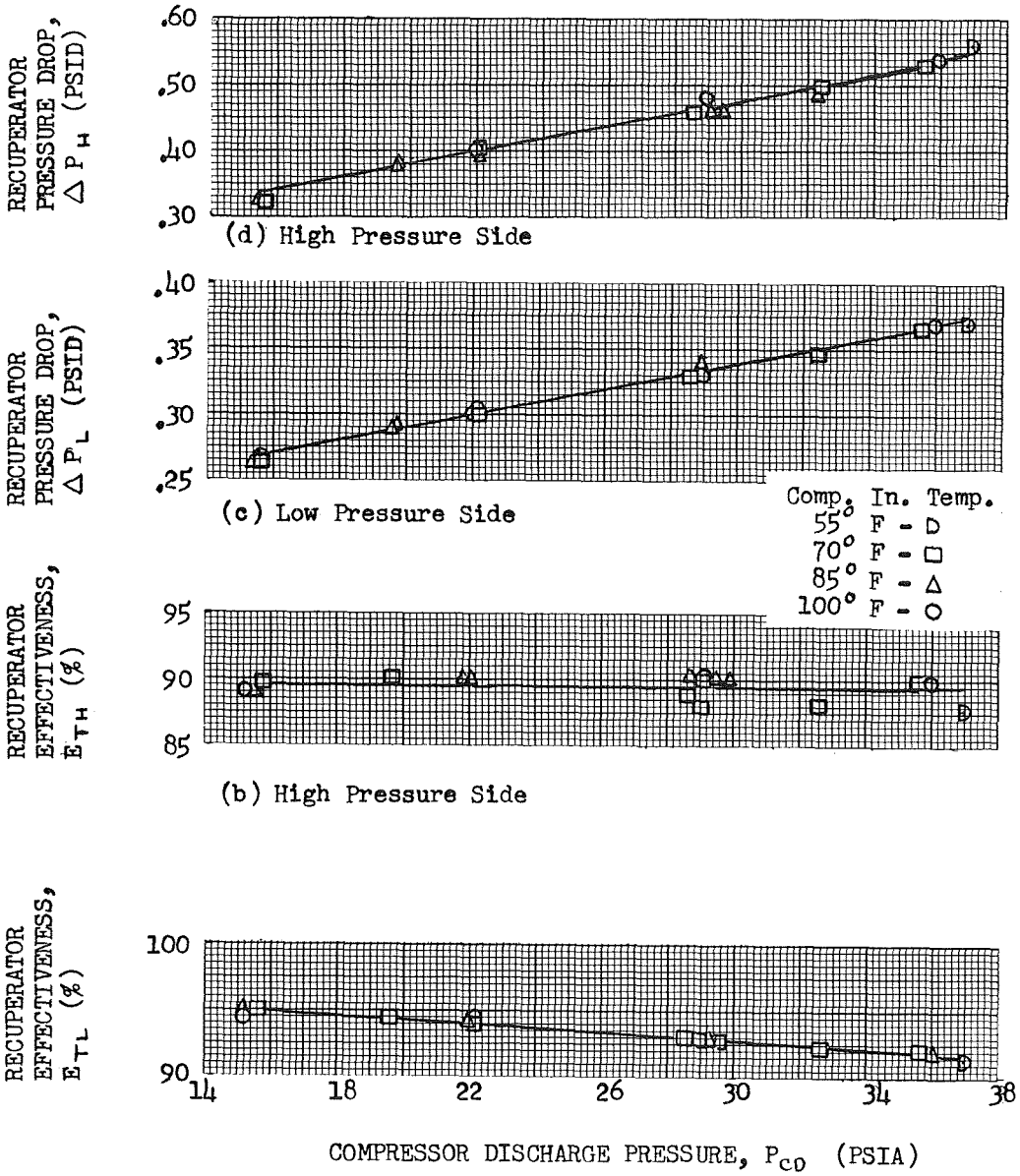

Figure 14: Variation of Recuperator Pressure Drop and Recuperator Temperature Effectiveness with Compressor Discharge Pressure at Turbine Inlet Temperature of 1600° F. Krypton Gas

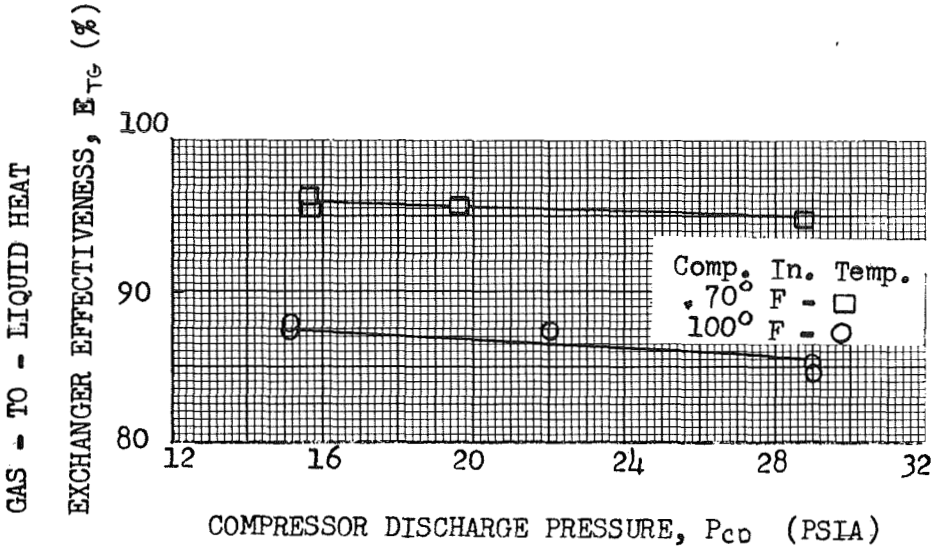

Figure 15: Effects of Discharge Pressure on the temperature effectiveness of the gas side of The Waste Heat- Heat Exchanger, Turbine Inlet Temperature = 1600° F. Krypton Gas

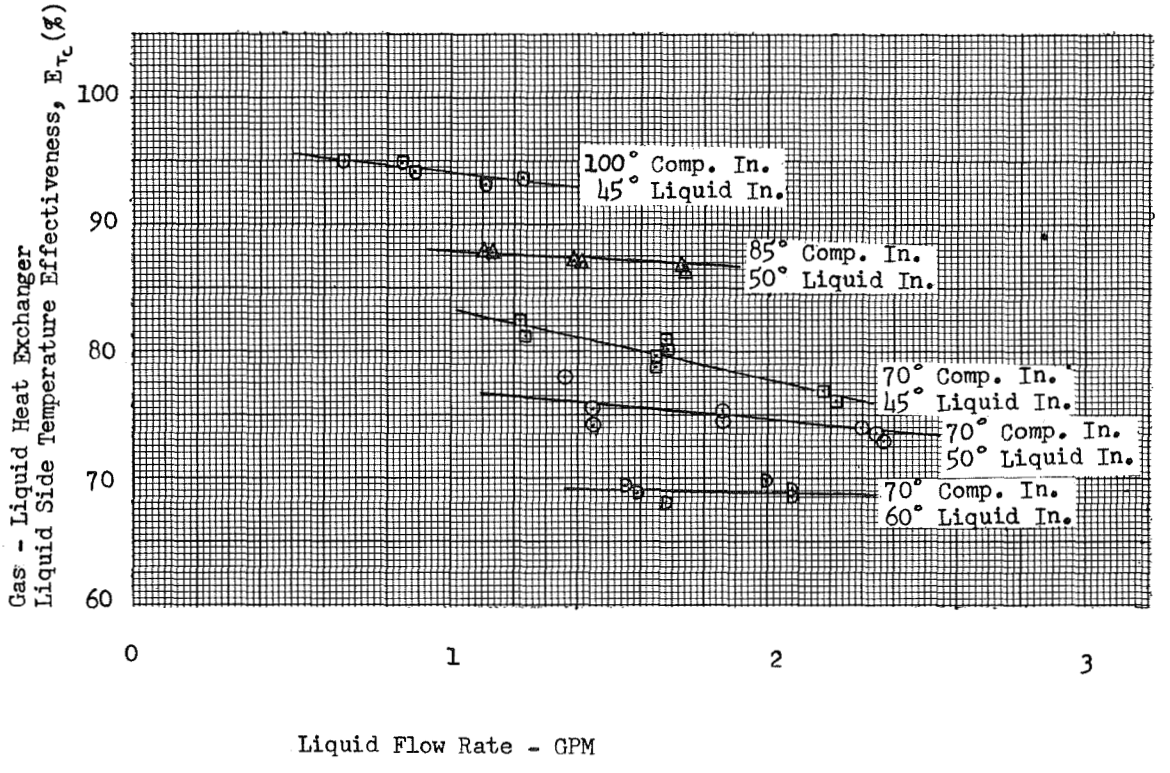

Figure 16 : Effect of coolant flow rate on the waste heat heat-exchanger, liquid side temperature effectiveness. Krypton Gas

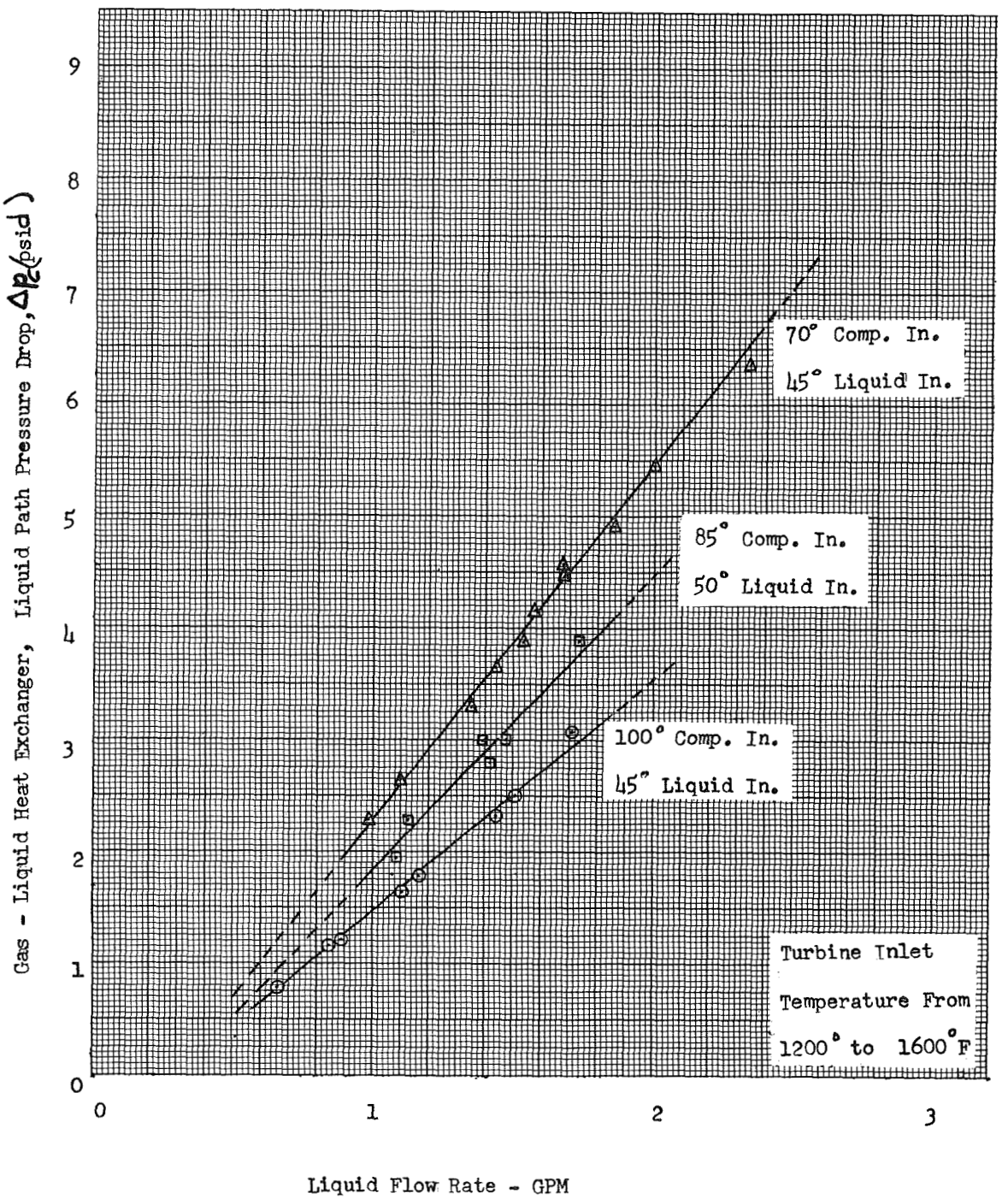

Figure 17: Effect of coolant flow rate on the waste heat heat-exchanger, pressure drop . Krypton Gas

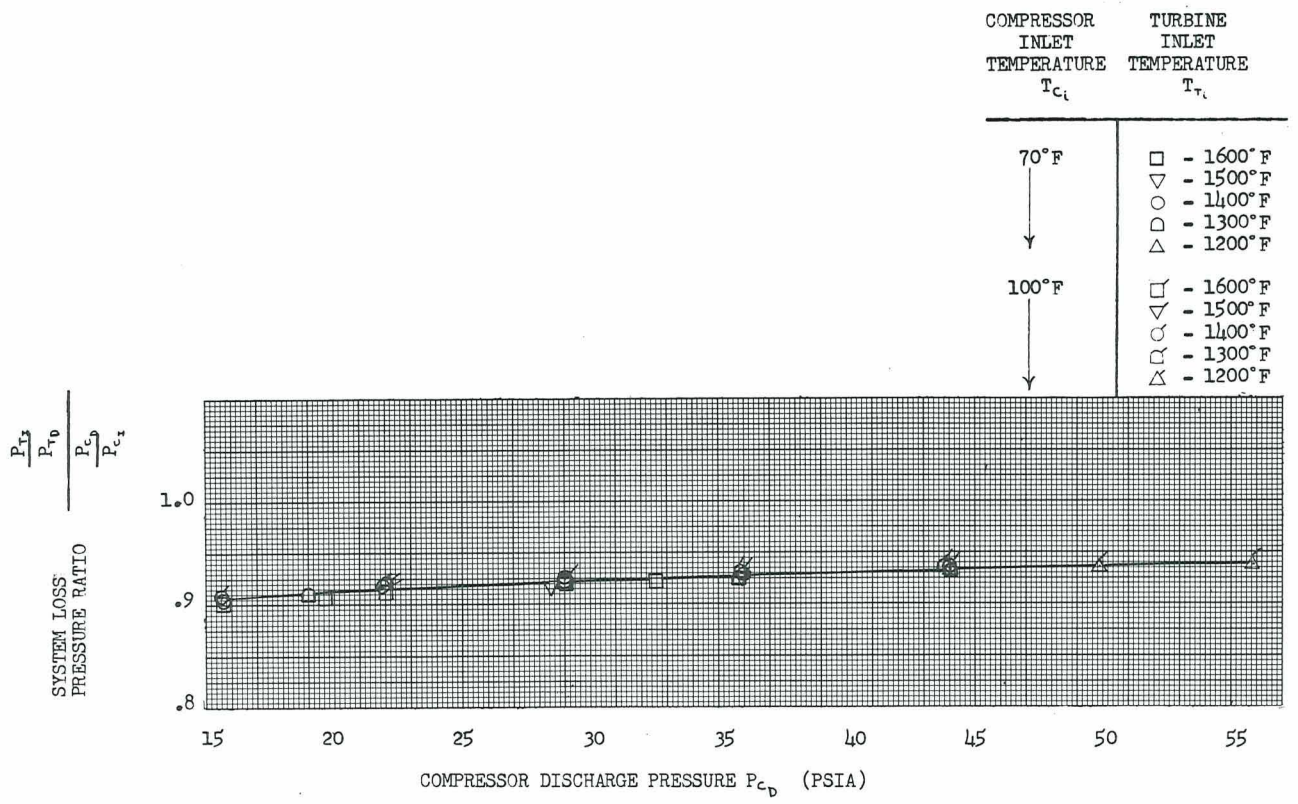

Figure 18 : Variation of system loss pressure ratio with compressor discharge pressure. Krypton Gas

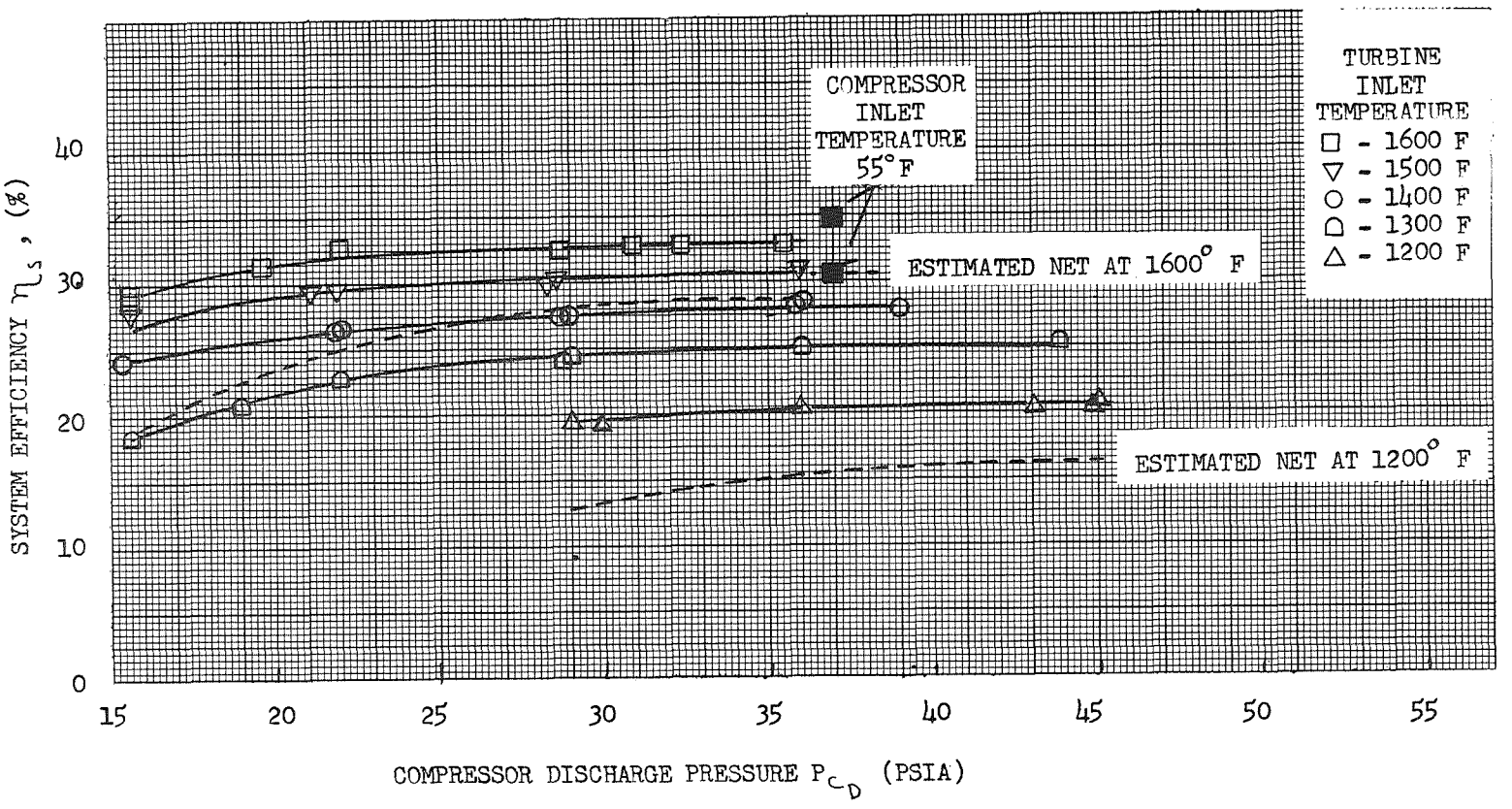

Figure 19 : Effect of compressor discharge pressure on system efficiency. Krypton Gas

(a) Compressor inlet temperature = 70°F

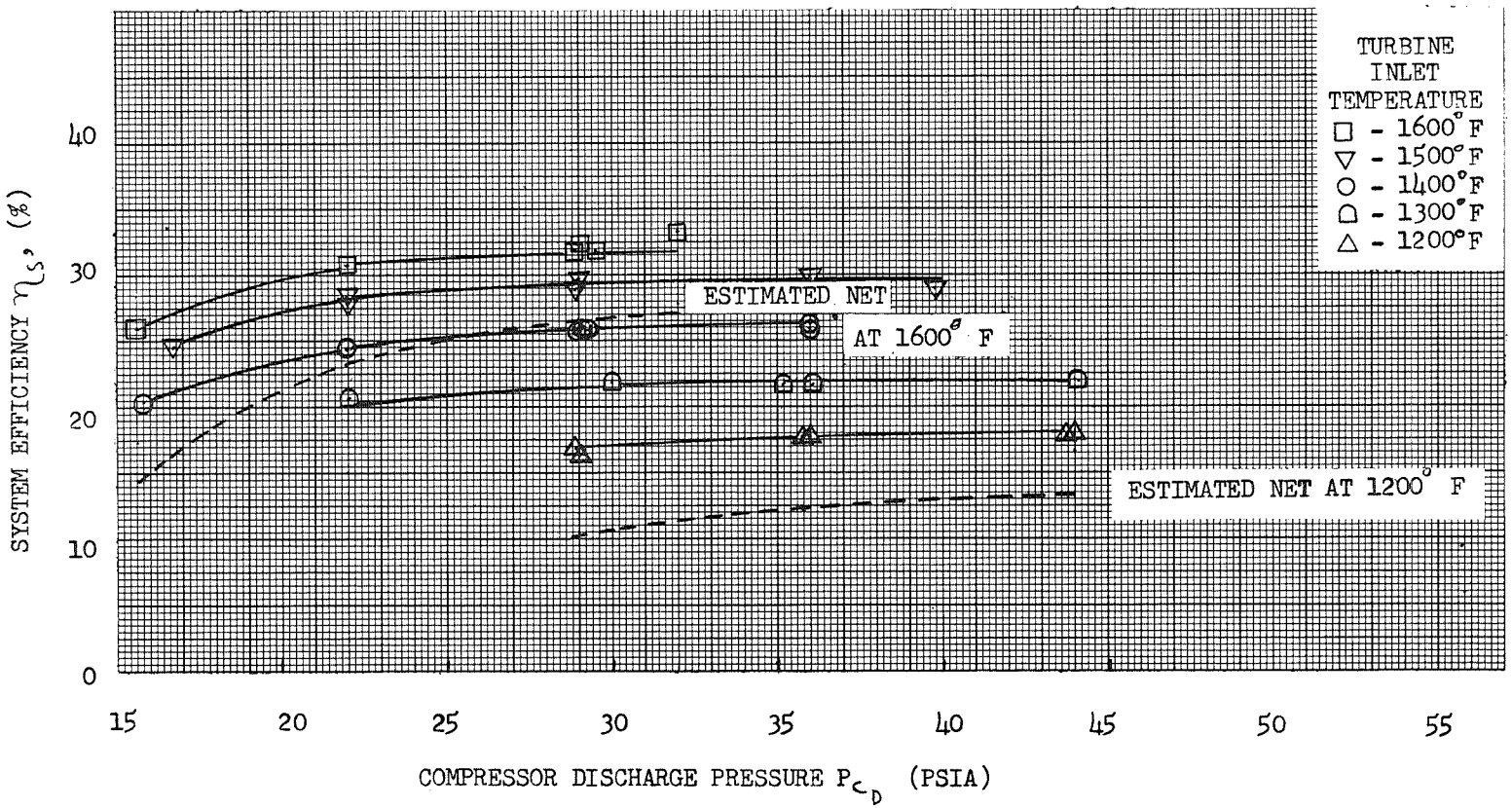

Figure 19 : Continued. (b) Compressor inlet temperature = 85°F. Krypton Gas

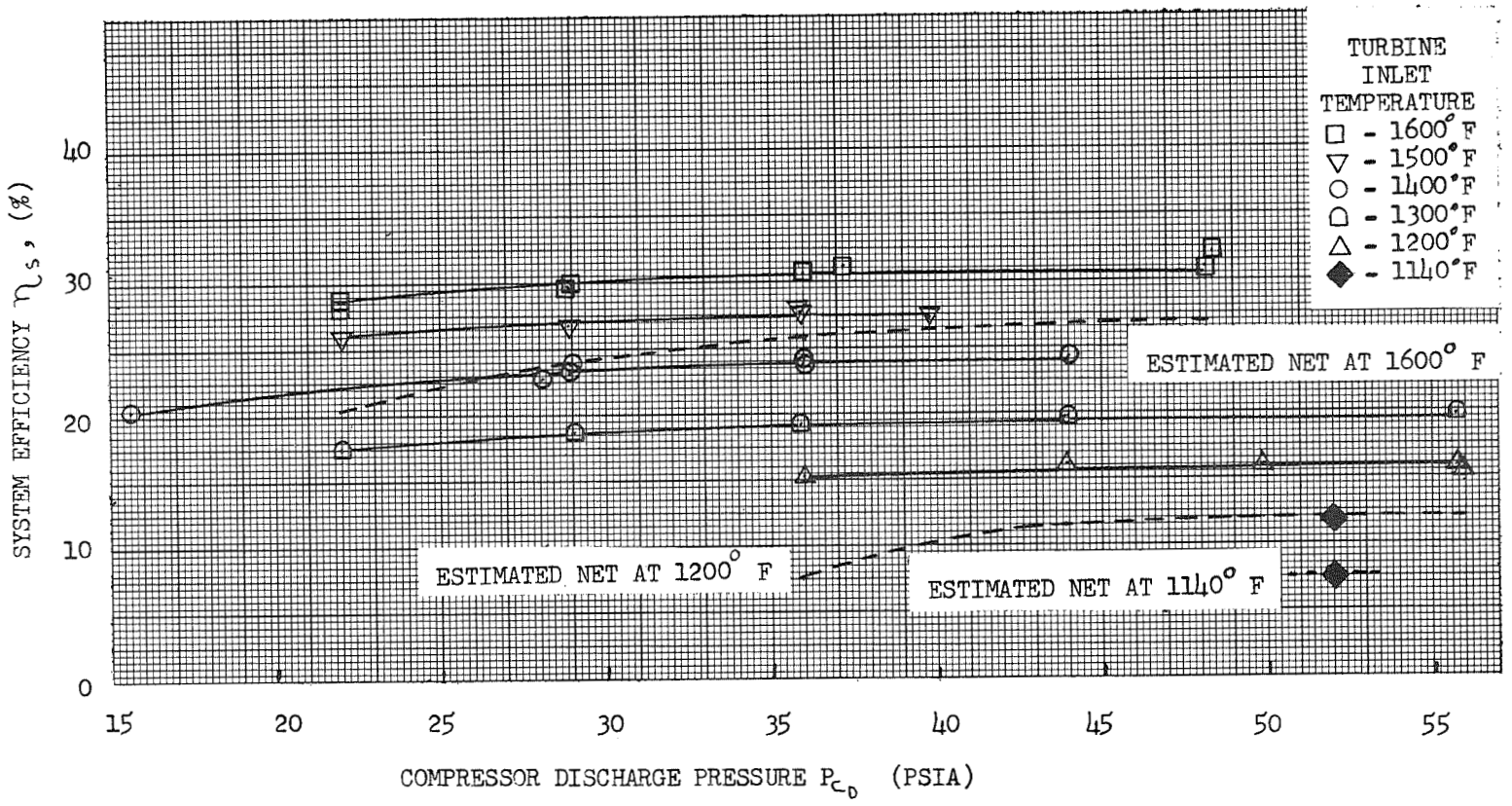

Figure 19 : Concluded. (c) Compressor inlet temperature = 100°F, Krypton Gas